**Kaunas University of Technology**

**Faculty of Mechanical Engineering and Design**

# Non-Destructive Evaluation of Honeycomb Sandwich Using Ultrasonic Phased Arrays

Final project for master's degree

Mastan Raja Papanaboina

**Project author**

Prof . Dr. Elena Jasiūnienė

**Supervisor**

**Kaunas, 2019**

**Kaunas University of Technology**

**Faculty of Mechanical Engineering and Design**

# Non-Destructive Evaluation of Honeycomb Sandwich using Ultrasonic Phased Arrays

Final project for master’s degree

Aeronautical Engineering(6211EX024)

**Mastan Raja Papanaboina**

Project author

**Prof . Dr. Elena Jasiūnienė**

Supervisor

**Prof . Dr. Rimašauskienė Rūta**

Reviewer

**Kaunas, 2019**

Kaunas University of Technology

Faculty of Mechanical Engineering and Design

(Faculty)

Mastan Raja Papanaboina

(Students name, surname)

Aeronautical Engineering (6211EX024)

(Tittle and code of study program)

# Non-Destructive Evaluation of Honeycomb Sandwich using Ultrasonic Phased Arrays

Declaration of Academic Honesty

___ ____ ________

Kaunas

I confirm that a final project by me, **Mastan Raja Papanaboina**, on the subject " Non-Destructive Evaluation of Honeycomb Sandwich using Ultrasonic Phased Arrays" is written completely by myself; all provided data and research results are correct and obtained honestly. None of the parts of this thesis have been plagiarized from any printed or Internet sources, all direct and indirect quotations from other resources are indicated in literature references. No monetary amounts not provided for by law have been paid to anyone for this thesis.

I fully and completely understand that any discovery of any manifestations/case/facts of dishonesty inevitably results in me incurring a penalty according to the procedure(s) effective at Kaunas University of Technology.

(name and surname filled in by hand) (signature)

**Kaunas University of Technology**

**Faculty of Mechanical Engineering and Design**

Study Programme – Aeronautical Engineering 6211EX024

**Task Assignment for Final Degree Project of Master Studies**

**Student**: Mastan Raja Papanaboina

**1. Title of the Final Project:**

Non-Destructive Evaluation of honeycomb sandwich using ultrasonic phased arrays

Korinio kompozito neardomoji kontrolė naudojant ultragarsines fazuotas gardeles

**2. Aim of the Final Project:**

The aim of the thesis is the investigation and evaluation of honeycomb sandwich material defects using non- destructive ultrasonic phased arrays.

**3. Tasks of the Final Project:**

- To study different types of defects and NDT methods on carbon fiber honeycomb panel.
- To determine the most suitable ultrasonic NDT technique and its parameters for inspection of carbon fiber sandwich panel by CIVA computational software.
- To perform investigation of ultrasonic wave propagation in sample with and without defects using Abaqus.
- To perform the experimental investigation, using parameters obtained by CIVA.

**4. Structure of the Text Part:** Liturature, analysis, experiments and conclusions

**5. Consultants of the Final Project:**

**Author of the Final Project** Mastan Raja Papanaboina
*(Name, Surname, Signature, date)*

**Supervisor of the Final Project** Prof . Dr. Elena Jasiūnienė
*(Name, Surname, Signature, date)*

**Head of Study Programme** Janina Jablonskytė
*(Name, Surname, Signature, date)*

Mastan Raja Papanaboina, Non-Destructive Evaluation of Honeycomb Sandwich using Ultrasonic Phased Arrays. The final project for *master's degree* / supervisor Prof. Dr. Elena Jasiuniene; Kaunas University of Technology, Faculty of mechanical engineering and design, department of transport engineering.

Study field and area (study field group): Aeronautical Engineering (E14), Engineering Science.

**Keywords**: Ultrasonic technology, non-destructive test, delamination defects, CIVA computational software, finite element method, ultrasonic phased arrays, transducer.

Kaunas, 2019. 66 p.

## SUMMARY

The objective of this thesis is determination of defects in honeycomb sandwich material using ultrasonic phased arrays. The computational parameters set back to conduct investigations on real-time experiments. The CIVA computer results are helps to obtain the desired parameters to follow the experimental estimation. The computer-aided design model was designed, and the finite element method simulation conducted to demonstrate the ultrasound wave propagation on the carbon fiber material with defect and without defect. The experimental analysis conducted and the defect on the sample was detected. The different frequency ranges 3.5 and 5 MHz with different transducers are helped to differentiate the defect positions and sizes. The different scan views are obtained to understand the defects in the sample. The conclusions are drawn the capability of a transducer and ultrasonic promising techniques which can identify defects precisely.

Mastan Raja Papanaboina. " Korinio kompozito neardomoji kontrolė naudojant ultragarsines fazuotas gardeles ". Magistro studijų baigiamasis projektas / vadovė prof. dr. Elena Jasiūnienė; Kauno technologijos universitetas, Mechanikos inžinerijos ir dizaino fakultetas.

Studijų kryptis ir sritis (studijų krypčių grupė): Aeronautikos inžinerija (E14), Inžinerijos mokslai.

**Raktiniai žodžiai**: Ultragarsinė technologija, neardomieji bandymai, defektų defektai, CIVA skaičiavimo programinė įranga, baigtinių elementų metodas, ultragarso fazinės matricos, keitiklis.

Kaunas, 2019. 66 p.

## SANTRAUKA

Šio darbo tikslas yra defektų korinio anglies pluošto kompozite aptikimas panaudojant ultragarsines fazuotas gardeles. Buvo sukurtas kompiuterinis modelis ir buvo atliktas modeliavimas naudojant CIVA programinę įrangą ir baigtinių elementų metodą siekiant ištirti ultragarso bangų sklidimą anglies pluošto kompozite be defektų ir su defektais. Darbe pateikiami ultragarsinės bangos sąveikos su bandinio defektais rezultatai. Atlikta eksperimentinė analizė. Tyrime naudoti skirtingų dažnių 3,5 ir 5 MHz fazuotos gardelės. Darbe parodyta, kad naudojant linijines fazuotas gardeles, galima įvertinti korinio kompozito kokybę.

# Table of Contents

**1. INTRODUCTION** ..... **11**

**2. THE CASE STUDY ON COMPOSITE MATERIALS AND DEFECTS IN CFSM** ..... **12**

2.1 CARBON FIBER REINFORCED POLYMER (CFRP) ..... 12

2.2 CARBON FIBER SANDWICH MATERIAL ..... 13

2.3 NATURE OF DAMAGES IN COMPOSITE MATERIAL ..... 14

2.4 EVALUATION OF NON-DESTRUCTIVE METHODS ON CARBON FIBER SANDWICH MATERIAL ..... 18

2.4.2 Infrared/Thermal test ..... 19
2.4.3 Visual test ..... 19
2.4.4 Eddy current test ..... 19
2.4.5 Magnetic particle test ..... 20
2.4.6 Liquid penetrate test ..... 20
2.4.7 Ultrasonic method ..... 20

2.5 ANALYSIS OF ULTRASONIC TECHNIQUES ON CARBON FIBER SANDWICH MATERIAL ..... 23

2.5.1 Air coupled method ..... 23
2.5.2 Through transmission ..... 24
2.5.3 Pulse-echo Phased Array ..... 25

2.6 EVALUATION OF DIFFERENT TYPES OF TRANSDUCERS ..... 25

2.7 Conclusion ..... 29

**3. CIVA COMPUTER MODELING AND ANALYSIS ON CARBON FIBER MATERIAL** ..... **30**

3.1 CIVA simulation set-up ..... 30

3.2 THE CIVA COMPUTATIONAL RESULTS ..... 36

3.3 CARBON FIBER SANDWICH MODELLING IN CIVA ..... 39

3.4 CIVA CONCLUSIONS ..... 42

**4. CAD AND FEM MODELING** ..... **43**

4.1 FINITE ELEMENT METHOD MODELLING ..... 45

4.2 FINITE ELEMENT METHOD RESULTS ..... 46

4.3 CONCLUSION OF ANALYSIS USING THE FINITE ELEMENT METHOD ..... 49

**5. EXPERIMENTAL ANALYSIS OF DEFECTS ON CARBON FIBER SANDWICH MATERIAL** ..... **51**

5.1 TRANSDUCERS ..... 51

5.1.1 Single transducer inspection ..... 52
5.1.2 Linear array transducer inspection ..... 54

5.3 EXPERIMENTAL CONCLUSIONS ..... 57

6. CONCLUSION ..... 58

**7. REFERENCES** ..... **59**

8. APPENDIX ........................................................................................................ 62

# List of abbreviations

**CFRP**: Carbon fiber reinforced polymer

**CFSM**: Carbon fiber sandwich material

**NDT**: Non-destructive testing

**NDE**: Non-destructive evaluation

**FEM**: Finite element method

**CAD**: Computer-aided design

**CAE**: Computer-aided engineering

# List of Figures

**Fig 1**. Carbon fiber sandwich material[2]. 14
**Fig 2**. The small disbond in carbon fiber honeycomb sandwich panel [4]. 15
**Fig 3**. The detachment of skin due to poor bonding quality [4]. 15
**Fig 4**. The delamination defect between two ply of carbon fiber skin [5]. 16
**Fig 5** (a), (b), (c). Honeycomb cell wall damage using impactor [6]. 16
**Fig 6**. Evolution of impact damage in different core thickness material using impactor [6]. 17
**Fig 7**. X-ray view of the honeycomb sample with impact damages. 19
**Fig 8**. Ultrasound wave propagation on the material. 20
**Fig 9**. Experiment set-up for the through transmission. 21
**Fig 10**. Longitudinal and shear wave behavior [7]. 22
**Fig 11**. C-scan view of air-coupled investigation [9]. 23
**Fig 12**. through transmission configuration [23]. 24
**Fig 13**. On field air-coupled through transmission investigation [9]. 24
**Fig 14**. Dual element transducer set-up [20]. 25
**Fig 15**. Angle beam transducer set-up. 26
**Fig 16**. The single element transducer set-up. 26
**Fig 17**. Linear array transducer elements. 28
**Fig 18**. Ultrasonic wave diffraction due to velocity change [21]. 28
**Fig 19**. The simulation set-up on carbon fiber skin and core. 30
**Fig 20**. The simulation set-up of a sandwich structure with carbon fiber skin and core. 31
**Fig 21**. simulation setup on sample in CIVA. 34
**Fig 22**. the placement of defects with different configuration. 36
**Fig 23**. Scan view of identified defects with different depth using 3.5 MHz frequency. 37
**Fig 24**. A- scan view of the three defects placed on sample analyzed with 3.5 MHz 37
**Fig 25**. Scan view of identified defects with depth using 5 MHz frequency. 38
**Fig 26**. The A-scan view of the defects on sample with 5MHz frequency. 39
**Fig 27**. Composite model and analysis set-up. 39
**Fig 28**. The placement of defects with different sizes. 40
**Fig 29**. Scan view of defects on model. 41
**Fig 30**. A- scan view of defects amplitude. 41
**Fig 31**. The geometry of composite skin. 43
**Fig 32**. Carbon fiber honeycomb sample for FEM. 44
**Fig 33**. The carbon fiber skin with defect. 45
**Fig 34**. The Mesh attribution in Abaqus explicit. 46
**Fig 35**. The wave propagation without defect. 46
**Fig 36**. Wave propagation on defect area. 47
**Fig 37**. Displacement of wave distribution path on defect-free zone. 48
**Fig 38**. Displacement of wave distribution path on defect zone. 49
**Fig 39**. Carbon fiber honeycomb sandwich sample. 51
**Fig 40**. Experimental setup of a single element transducer. 53
**Fig 41**. Practical experimental set-up using a single element transducer. 53
**Fig 42**. Single element transducer wave display on CFSM. 54
**Fig 43**. The experimental setup of the linear transducer array. 55
**Fig 44**. The linear transducer array result of carbon fiber sandwich material. 55
**Fig 45**. Linear transducer array detected damage on scan view. 56
**Fig 46**. Experimental results with 3.5 MHz 56
**Fig 47**. Experimental results with 5 MHz 57

# List of Tables

TABLE 1. NATURE OF DAMAGE AND SUITABLE NDT METHOD ..... 14
TABLE 2. CONTACT AND NON-CONTACT METHODS..... 18
TABLE 3. THE TYPE OF ULTRASOUND WAVES. ..... 22
TABLE 4. FREQUENCY RANGE AND PIEZO ELEMENT SIZE. ..... 27
TABLE 5. PARAMETERS OF THE PROBE. ..... 27
TABLE 6. SPECIMEN PARAMETERS..... 31
TABLE 7. THE MATERIAL PROPERTIES CIVA SPECIMEN. ..... 33
TABLE 8. THE TRANSDUCER CRYSTAL SHAPE PARAMETERS. ..... 34
TABLE 9. COMPUTATIONAL SETTINGS IN CIVA SOFTWARE. ..... 35
TABLE 10. DEFECT PARAMETERS. ..... 40
TABLE 11. SINGLE ELEMENT TRANSDUCER SPECIFICATIONS. ..... 51
TABLE 12. LINEAR TRANSDUCER ARRAY PROPERTIES ..... 52

## 1. Introduction

In the contemporary world with emerging technologies, new composite materials are developed, honeycomb sandwich material is one of them. The advantageous qualities of honeycomb structure like high strength to weight ratio, resistance of fatigue, high bending resistance and light weight, play an important role in aerospace, automobiles and other engineering fields. The main concentration here is the application of honeycomb sandwich material in the field of aerospace. In aircrafts, the honeycomb sandwich materials are mostly used in rudder, flaps spoiler and aileron. These parts of the aircrafts are prone to impact damages due to point loads. This damage causes delamination between skin and core material of the honeycomb sandwich material[1]. These damages may cause catastrophic structural failures of the aircraft; hence analysis of delamination defects becomes important.

Non-Destructive testing is the investigation of material with existing technology that does not damage the material integrity or properties. Composite materials usage is growing extensively in the aerospace and automobile industries due to its high strength and weight ratio. In NDT field various technologies and methods are involved to deal with the internal and external abnormalities of the composite (CFRP and GPRP) or other materials. Non-destructive test helps to identify defects on composite materials after manufacturing and during the maintenance. The composite material composition, properties and geometric nature are obtained during the non-destructive test. It is cost effective and quality control technique. The ultrasound is the sound energy with frequency of higher than human capable of being heard range.

The Carbon fiber honeycomb materials can be investigated using air-coupled and immersion method, but the ultrasonic pulse-echo method is one the best way to identify the defects using single side access of the test section. The previous immersion method investigations on carbon fiber honeycomb sandwich panels reported that the additional problems occur like water ingression into the sample due to immersion of sample in the water tank. Ultrasound equipment work with different frequencies ranges based on the application of inspection, the frequency range starts from 20 kHz up to several megahertz[2]. The air-coupled ultrasound investigations are done with pitch-catch and through transmission using lamb waves but the pulse-echo method is also one of the technique which uses longitudinal waves to investigate the defects on carbon fiber sandwich material [3]. The following thesis report gives the capability of ultrasound pulse-echo technique using linear phased array. The proposed technique gives the defect detection of carbon fiber sandwich material.

The Objective of this thesis is investigation and evaluation of honeycomb sandwich material defects using non- destructive ultrasonic phased arrays. The following tasks are:

- To study different types of defects in carbon fiber honeycomb panel.
- To study different types of defects and NDT methods on carbon fiber honeycomb panel.
- To determine the most suitable ultrasonic NDT technique and its parameters for inspection of carbon fiber sandwich panel by CIVA computational software.
- To perform investigation of ultrasonic wave propagation in sample with and without defects using Abaqus.

To perform the experimental investigation, using parameters obtained by CIVA. To perform the experimental investigation, using parameters obtained by CIVA. The CIVA computer software was used for the initial steps of modeling the sample and analyzing it. Ultrasonic inspections were carried out on the computer-generated design of the sample using a phased array transducer with different frequency range. The appropriate frequency range was selected based on the obtained results of CIVA simulation. The sample selected was a honeycomb carbon fiber sandwich on which the experimental analysis was carried out using the ultrasonic technique. The impact damages on the honeycomb carbon fiber sandwich were detected by Omni scan measurement system and using linear phased array transducer.

The 2D model of carbon fiber reinforced plate with delamination type defects was prepared using Abaqus explicit in finite element method (FEM) software. Using CIVA simulation software the ultrasonic scan results are obtained for the delamination type defects between the composite layer which are created artificially.

The practical experiments are conducted to find the delamination defects between the two layers of the specimen. The simulation results are of great help in designing, selecting the appropriate inspection method and their qualification to identify the defects or to analyze it while reducing the number of physical trials and mock-ups. A lot of validation efforts have been put around the CIVA software to give evidence of model's validity to consider as a reliable element to support technical decisions and justifications.

High-end parametric analysis is essential in identifying the parameters that affect the performance of NDE. This analysis with purely experimental results should have access to large amount of data which makes it difficult and cost effective. Probability of detection methods, that links the probability to detect a detrimental flaw to its size is generally used for NDE reliability evaluation in the aerospace sector.

The honeycomb carbon fiber sandwich material is selected to analyze the small impact damages and size of the damages precisely. There are few other NDT techniques that are available to test the material, but the ultrasonic method is accurate with small impact damages and it is a cost effective and reliable.

## 2. The case study on composite materials and defects in CFSM

### 2.1 Carbon fiber reinforced polymer (CFRP)

In general, composites are made up of two elements, one is matrix, and the other is reinforcement. The matrix is resin to hold the fiber together and reinforcement material is fiber to give strength to the composite. Carbon fiber reinforced polymer, carbon fiber strengthened plastic or carbon fiber fortified thermoplastic are great solids with light fiber fortified plastics that consists of carbon strands[3,4]. CFRPs are quite expensive but are used when high strength-to-weight ratio and unbending nature are required like, aerospace, automobile, structural designing, racing sports and other applications. The elastic properties of the composite materials are estimated by the equation,

$$E_c = V_m . E_m + V_f . E_f \qquad (1)$$

Where,

$E_c$ = Modulus of total composite,

$V_m$ and $V_f$ = Volume fractions of matrix and fiber respectively,

$E_m$ and $E_f$ = Elastic moduli of matric and fiber, respectively.

### 2.2 Carbon fiber sandwich material

Composite materials are a combined product of two or more constituent materials to form physically or chemically strong component. In aircrafts, for primary structures these composite materials are being used frequently because of their superior strength properties than metallic materials[4]. In the contemporary world, composite materials are playing a key role in the aerospace sector and other engineering applications due to the superior qualities such as stiffness, high strength, lightweight. The fabrication of material is attaching two skins and the thick core. The honeycomb materials are mainly used where they need flat or slightly curve locations. The industries are mainly preferred honeycomb structures instead of carbon fiber reinforced polymer (CFRP) due to high specific strength, bending resistance and light weight makes the use in aerospace industry. In the aerospace sector, the different types of composite structures are used. The performance of commercial and military aircraft is constantly developing and improving with high-performance structural materials. In aerospace applications, high-performance automobiles, boats and wind turbines, sandwich panels play an important role in composite structure.

In composite, the volume of any element like fiber, matrix and overall composite is mass divided by the density[3]. The equation for the volume of composite is,

$$\frac{1}{\rho_C} = \frac{W_f}{\rho_f} + \frac{W_m}{\rho_m} \qquad (2)$$

If the density of composite material is computed, it is defined by weight fraction which is the product of density times volume.

$$W_f = \frac{\rho_f}{\rho_c} . V_f \qquad (3)$$

$$W_m = \frac{\rho_m}{\rho_c} . V_m \qquad (4)$$

Where,

$W_f$ and $W_m$ = Mass of the fiber and matrix,

$\rho_c$, $\rho_f$ and $\rho_m$ = Density of the composite, fiber and matrix.

Basically, the sandwich panel consists of outer skin layers which are made of stiff carbon fiber and an inner core made of low stiffness and low-density as shown in **Fig 1**. The whole structure is assembled by an adhesive material. The adhesive is the resin or coupling agent to making a strong bond between the skin and core [8,9].

There are different types of honeycomb structure material that can be used to fabricate the carbon fiber honeycomb sandwich material, but this material is manufactured with Nomex sheet. In general aluminum honeycomb structures are used in the previous decade. In order to reduce the additional weight Nomex sheets are used.

The carbon fiber honeycomb sandwich panels are widely used in the aeronautical field. These kinds of materials are used for cabin panel and control surface the aircraft. The control surfaces like rudder, aileron and spoilers.

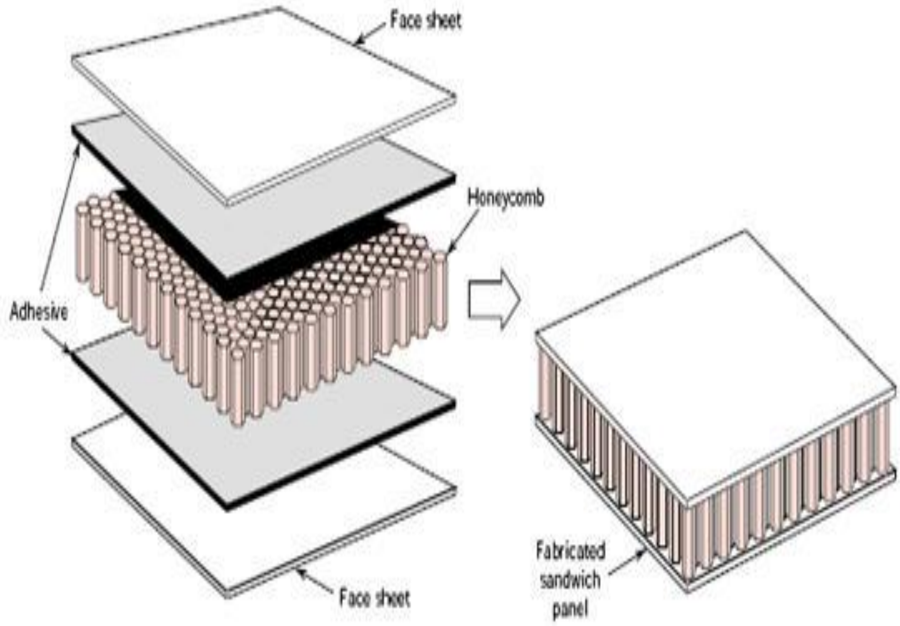


**Fig 1**. Carbon fiber sandwich material[2].

### 2.3 Nature of damages in composite material

Table 1 describes the most common defects encountered in composite structure. The main causes of damages and preferable NDT method to identify the flaws. The main aim of this research is finding, and estimating the delamination defect caused by the impact damage. The delamination defects are developed between the two layers of composite skin and core material. The space developed between the fiber layers occurs delamination [10,11].

Table 1. Nature of damage and suitable NDT method

| Type of defect | Causes for damage | Preferable NDT Method |
|---|---|---|
| Disbond | Manufacturer defect, Impact Damage | Ultrasonic method, Radiography |
| Delamination | Manufacturer defect | Radiography, Ultrasonic test and Tap Test |
| Porosity | Heat Damage (Lightning Strike) | Visual inspection, Magnetic particle test |
| Core Damage | Impact Damage | Radiography, Ultrasonic Test |

The *disbonding defect* is one the major problem in carbon fiber honeycomb sandwich panels, these types of defects are developing due to manufacturing failure, weak bond quality between skin and honeycomb structure and impact damage. The small disbond leads to detach the skin from the honeycomb structure due to cyclic loads and it damages the entire structure [12]. **Fig 2** shows that, the small defect developed due to poor quality of the bond between skin and honeycomb structure.

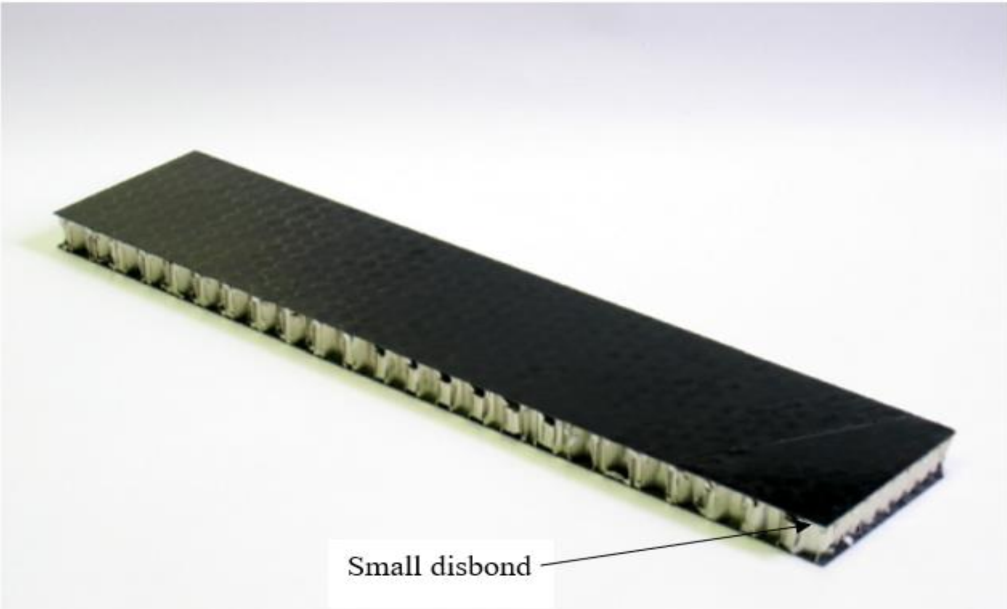


**Fig 2**. The small disbond in carbon fiber honeycomb sandwich panel [4].

The small disbond develops large defect due to cyclic load and then skin detached from the honeycomb structure. **Fig 3** shows the detachment of carbon fiber skin from the sandwich panel due to poor adhesive bond.

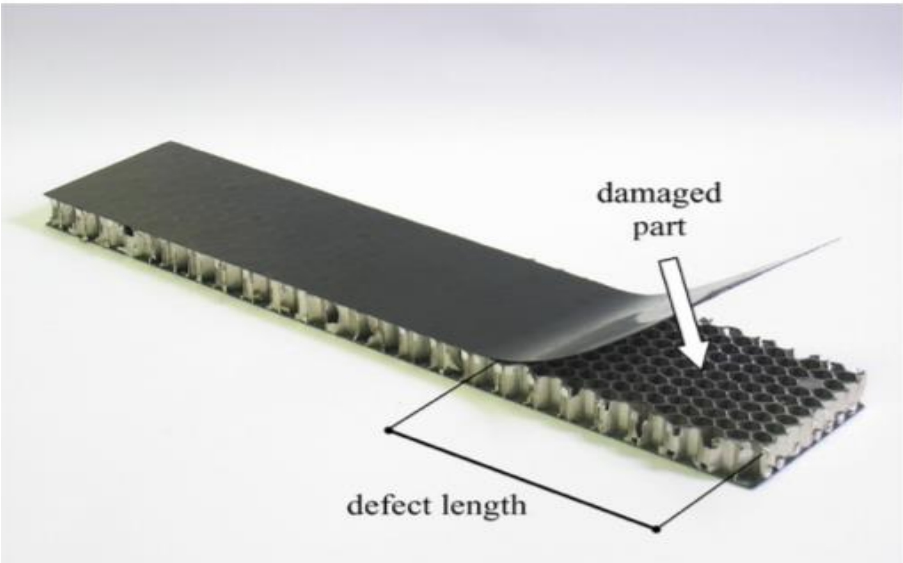


**Fig 3**. The detachment of skin due to poor bonding quality [4].

The ultrasonic phased array investigation is impressive technology to identify the defect at an early stage of the defect. The proof of defect detection on carbon fiber honeycomb sandwich panel presented in the experimental results of this thesis.

The *delamination defect* between the two plies of the carbon fiber composite is of major concern in the aeronautical structures. The small gap develops due to weak bond or load in two ply of composite creates delamination defect. The artificial delamination creates using Rosand Instrumented Falling Weight Impact Tester (IFWIT) on two ply composite material. The size of the delamination defect controlled by changing the height of the weight. **Fig 4** shows the ply carbon fiber material with different orientation. The top layer oriented with 45° and lower layer oriented with 90° and the 3-micrometer delamination appeared between two layers [5].

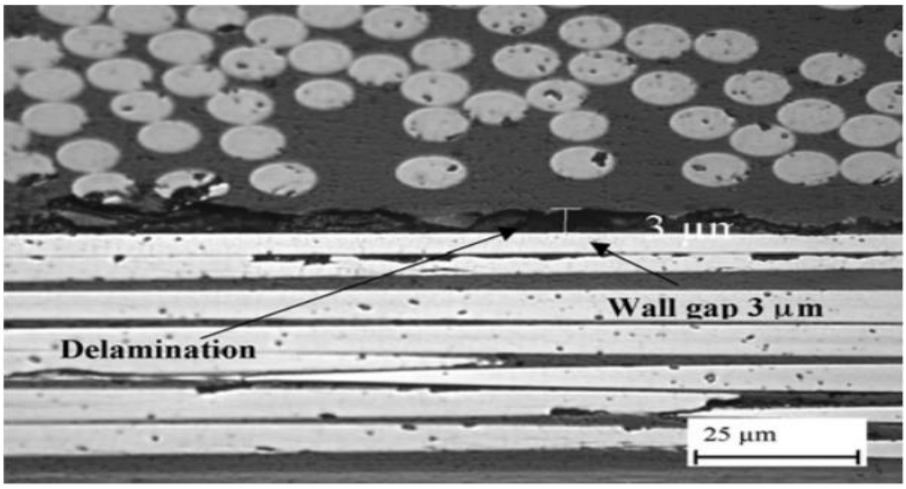


**Fig 4**. The delamination defect between two ply of carbon fiber skin [5].

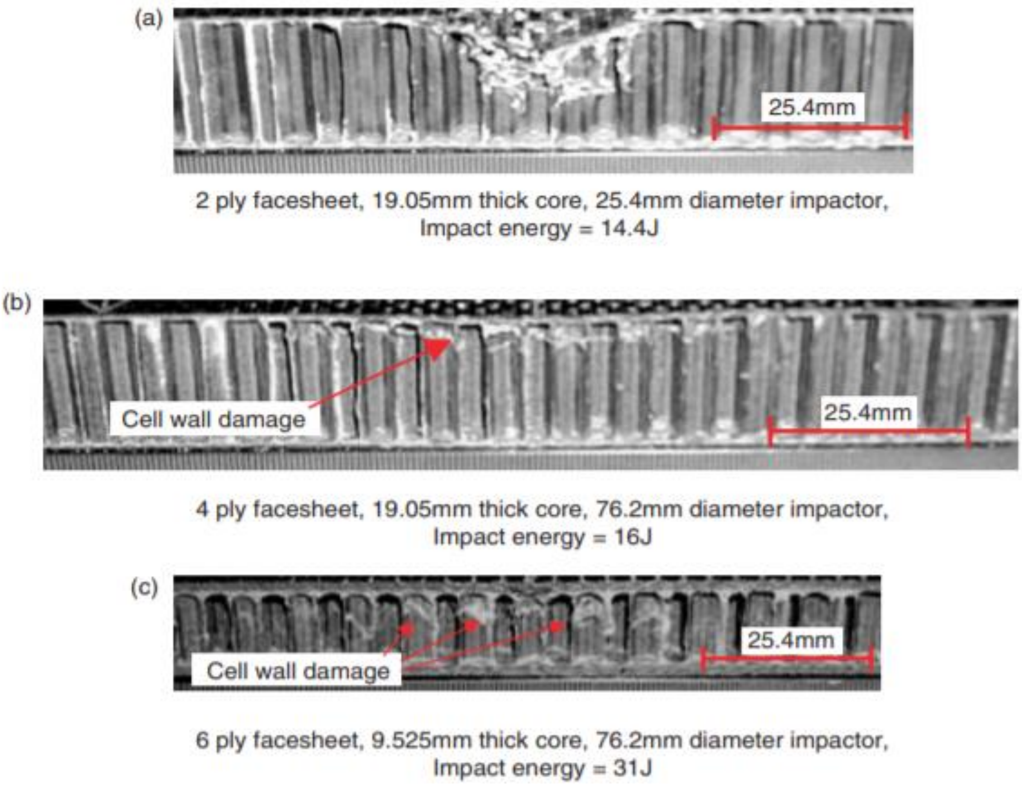


**Fig 5** (a), (b), (c). Honeycomb cell wall damage using impactor [6].

**Fig 5(a, b, c)** shows the different range impact energy applied on the specimen. In **Fig 5(a)** 14.4 joules energy used to create damage on two ply face sheet skin with 25.4 mm diameter of the impactor. In **Fig 5(b)** 16 joules energy used to create damage on four ply face sheet skin with 76.2 mm diameter of the impactor. In **Fig 5(c)** 31 joules of energy used to create damage on six face sheet skin with 76.2 mm diameter of the impactor [6].

The impact damage leads to the damage of the honeycomb structure (core). The honeycomb pattern was suppressed due to impact energy and it causes a dent in the core structure. The previous investigations are carried on carbon fiber honeycomb sandwich material and the experimental results with ultrasonic through-transmission method are obtained. The artificial damages were created with impactor on different ply face sheet of the honeycomb structure [13].

The **Fig 6** shows the carbon fiber skin and core damage ignition, damage progression, skin fracture, top skin penetration and honeycomb core structure fracture, skin, core damage and damage penetration to bottom skin. The different thickness of honeycomb sample is evolved with manual impactor [14].

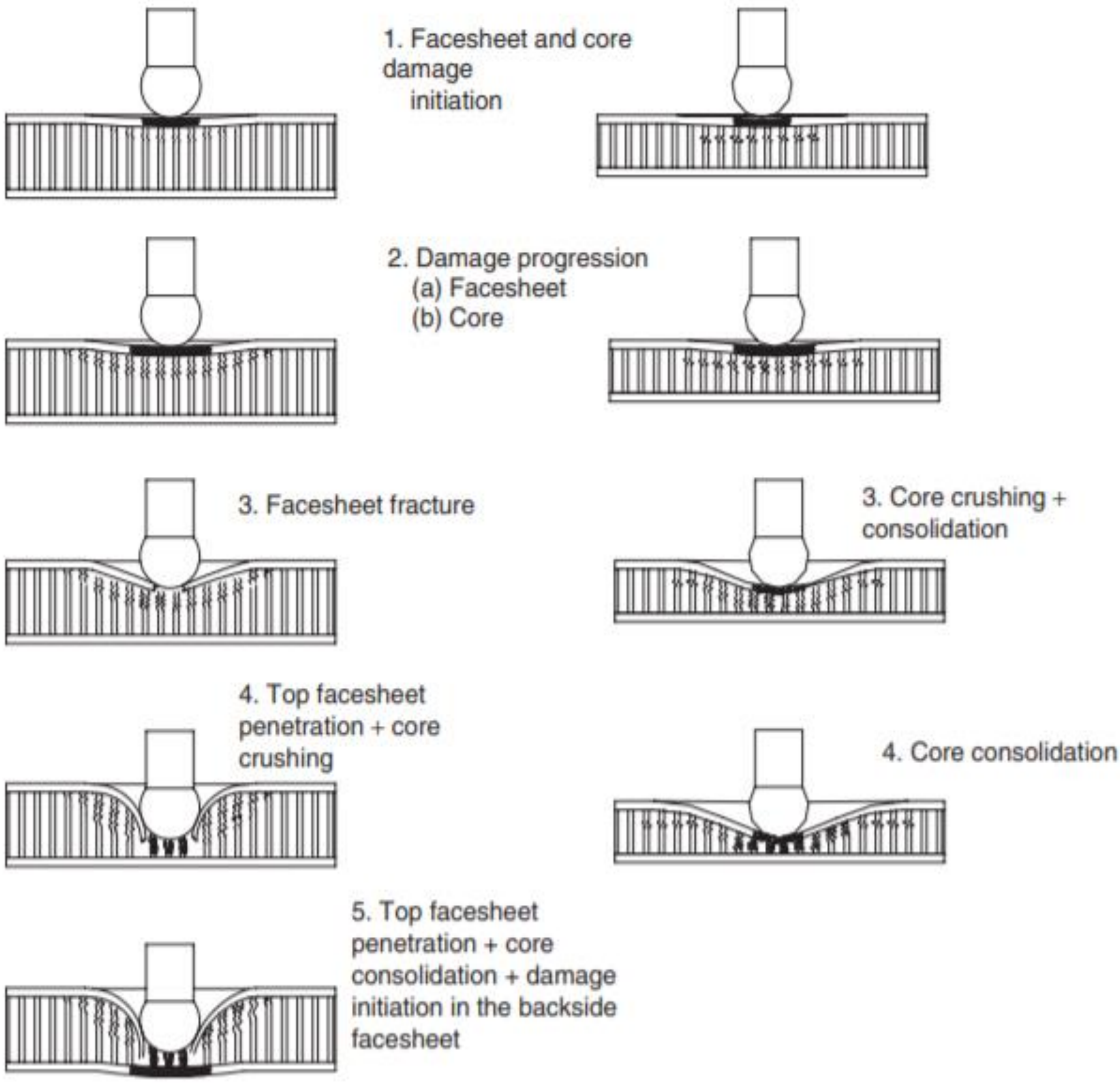


**Fig 6**. Evolution of impact damage in different core thickness material using impactor [6].

### 2.4 Evaluation of Non-destructive methods on carbon fiber sandwich material

There are different types of NDT techniques each technique having its own unique capability to detect the defects. The methods are [7,8],

- Ultrasonic test
- Radiography test
- Eddy current test
- Magnetic particle test
- Liquid penetrate test
- Visual test
- Thermal/infrared test
- Laser test
- Leak test
- Acoustic emission test
- Guided wave test
- Magnetic flux leakage test

There are two categories of NDT methods such as contact and non-contact methods. The contact methods are allowed to contact the surface of the specimen to identify the defects or properties of materials. In this method, the probe should have access to touch the surface of the test piece. Another method is non-contact method, those do not contact with the test piece [9]. In this method the frequency can travel through the air or water. To analyze the material, the inspector doesn't need to get in touch the specimen [15]. The type of contact methods and non-contact methods are displayed in table 2.

Table 2. Contact and Non-contact methods

| Contact Methods | Non-contact methods |
|---|---|
| Ultrasonic contact test | Ultrasonic Through transmission |
| Eddy Current Test | Radiography Test |
| Magnetic particle Test | Thermography Test |
| Liquid penetrate Test | Visual Test |
| Electromagnetic Test | Stereography Test |

#### 2.4.1 Radiography test

In real time application, radiography testing is more suitable for the impact damages on carbon fiber sandwich material. In this case, the impact damage on carbon fiber sandwich material is very small.

The experimental test has been done on material, but radiography test has been failed to capture the impact damage [10]. So, in this case, the ultrasonic method is suitable to detect the damage precisely. **Fig 7** shows the x-ray view of CFSM.

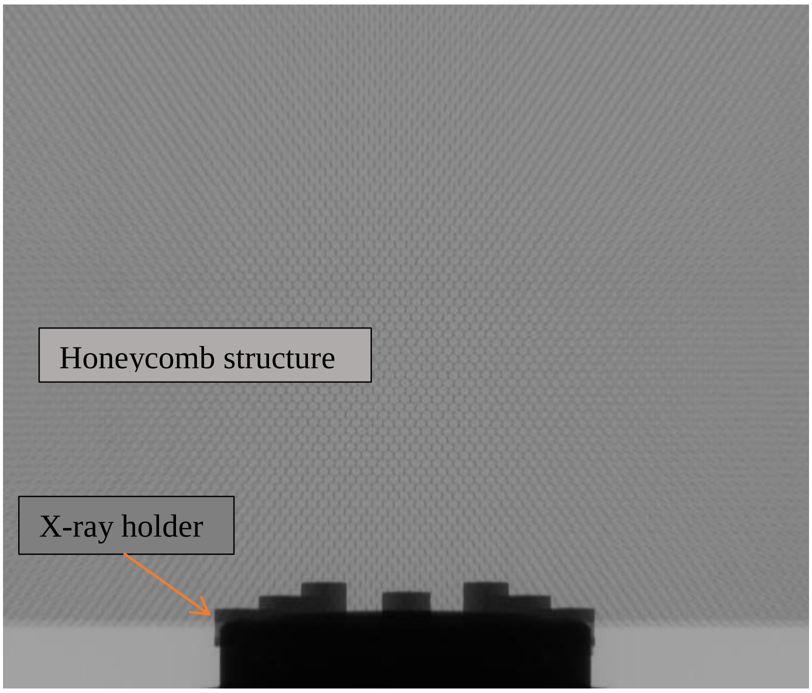


**Fig 7**. X-ray view of the honeycomb sample with impact damages.

### 2.4.2 Infrared/Thermal test

The thermal inspection is like the radiography test. The thermal images can be obtained during the test. In this case, there is a possibility to detect the impact damage. Thermal inspection is mainly used to detect the internal flaws in concrete structures such as bridges, buildings and highways.

When comparing the ultrasonic test with the thermal test, ultrasonic inspection is the simplest way to inspect the material without radiation and it is economical inspection compare to thermal inspection [15].

### 2.4.3 Visual test

Visual test is a great technique for the impact damage on the material. The visual inspection can be enhanced with the use of optical instruments such as mirrors, borescopes, magnifying glasses and fiberscopes. Let us consider the sample like honeycomb sandwich material with impact damage, the visual inspection can give only damage identification but cannot find the impact damage size accurately. But the ultrasonic technique with transducer array gives precise data of damage [16].

### 2.4.4 Eddy current test

The magnetic field is generated when an alternative current pass through the coil. Eddy currents are induced in the material when the probe is placed on the electrically conductive material. If there is any defect it disturbs the eddy current circulation. Based on the coil impedance variation inspector can identify the defect [17].

In the case of impact damages on carbon fiber sandwich material which is electrically non-conductive material. The current cannot pass through the carbon fiber material. The eddy current test depends on material conductivity. So, the eddy current is not suitable for the carbon fiber sandwich material.

### 2.4.5 Magnetic particle test

Magnetic particle testing can be done only on ferromagnetic materials like nickel, iron, gadolinium, cobalt and some alloys. In this case, the honeycomb carbon fiber sandwich material is not a ferromagnetic material. The magnetic particle testing is absolutely not suitable for the carbon fiber sandwich material.

### 2.4.6 Liquid penetrate test

The liquid penetrate inspection mainly used for surface cracks, porosity on the surface, surface weld defects and fatigue cracks. The penetrant can be applied by spraying on the surface of the test object. When the fluid is applied on the material, it will penetrate on the dry area. After some time, it is to remove the penetrant and the developer has to be applied [13]. Due to the developer penetrant comes out from the flaw. Inspector can see the flaw using ultraviolet light or under daylight.

In this case, fluid cannot penetrate into the surface. On carbon fiber sandwich material having the impact damages. The surface of the material cannot allow the fluid inside the material. The liquid penetrate test is completely not suitable for this particular defect [18].

### 2.4.7 Ultrasonic method

Considering all the above methods, the ultrasonic method would be the best possible method to analyze the carbon fiber sandwich material due to its advantages. Using ultrasonic method internal defects such as delamination between skin and core material can be validated with size and position.

One side access of the sample is enough for inspection, irrespective of the orientation of the cracks and volumetric defects can be detected and there is no radiation hazard while inspecting. In ultrasonic method the transducer generates low to high frequency ultrasonic energy. The ultrasonic energy travels from the transducer to object [19].

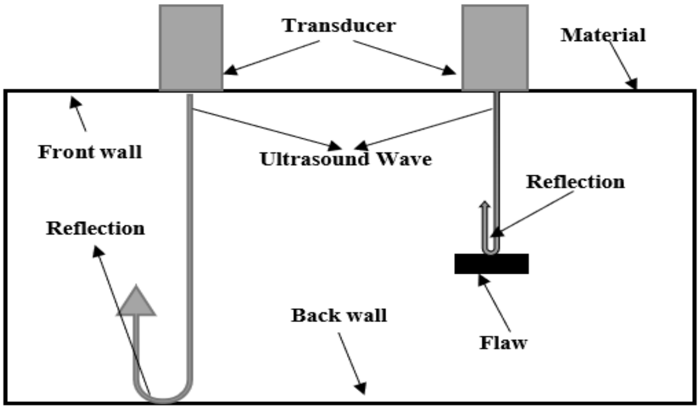


**Fig 8**. Ultrasound wave propagation on the material.

When the flaw is detected in the way of wave path, the ultrasonic wave travels back from the flaw. The setup of the ultrasonic test and transducer placement on the specimen is illustrated in **Fig 8**. The wave propagation in absence of defect and presence of defect is presented.

If there is no discontinuity or abnormalities in object the sound energy travels to back wall of the object and it will reach the transducer. The reflected sound energy transformed into an electrical signal through the transducer and is shown in the measurement system. On desktop of the system, inspector can see the different scan views.

The main parameters of the ultrasonic waves are ultrasound velocity, frequency and wavelength. The measurement of defect is estimate by time versus amplitude. The ultrasound velocity is dependent on material properties and is completely different in solid, liquid and gas. The wavelength of the frequency can be found according to the equation, the wavelength is equal to the acoustic velocity by frequency [20].

$$\lambda = \frac{C}{f} \tag{5}$$

Where,

λ = Wavelength,

C = Acoustic velocity,

f = Frequency.

In the ultrasound technique, there are different methods that are pulse-echo, through transmission and air-coupled. The sound energy can travel in air and water. In through transmission method, the material placed between the two transducers.

One transducer is to transmit the sound energy and another transducer is to receive the sound energy from the transmitter. **Fig 9** shows the set-up for the through transmission method.

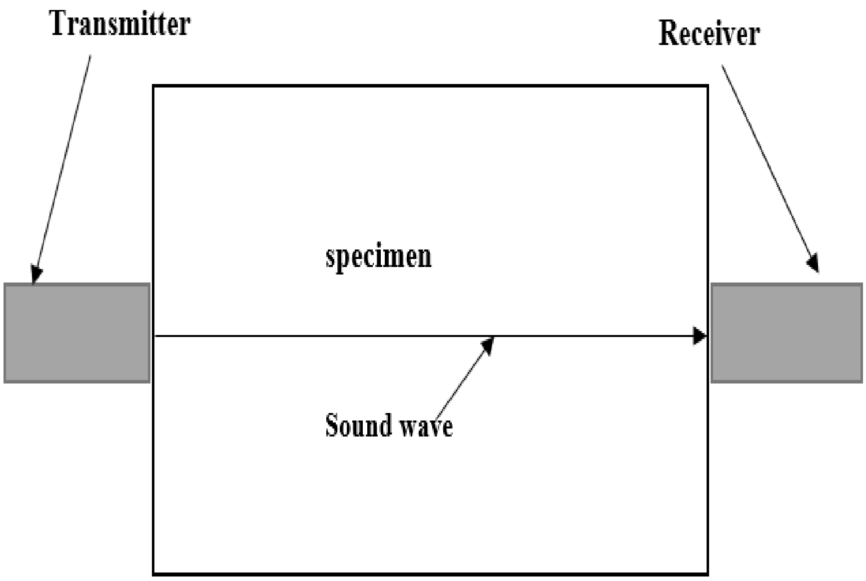


**Fig 9**. Experiment set-up for the through transmission.

Ultrasonic methods can be used in detecting the discontinuities, size of the defect and properties of the material. The ultrasonic wave velocity depends on solid based on elastic constants like Young's modulus, Poisson's ratio, Shear modulus, Lame's constants, Bulk modulus, Tensile modulus. The table 3 shows different types of ultrasound waves [21].

Table 3. The type of ultrasound waves.

| **Type of wave** | **Particle Vibration** |
|---|---|
| Longitudinal (Compression) | Parallel to wave direction |
| Transverse (Shear) | Perpendicular to wave direction |
| Surface (Rayleigh) | Elliptical orbit - symmetrical |
| Plate wave (Lamb) | Component perpendicular to surface |

Longitudinal wave is a type of wave which propagates from the ultrasound. The nature of the wave behavior is forth parallel to the direction of the wave propagation on investigating test specimen. These waves travel through any medium like air, water and solid with series of waves with compression and rarefaction mode. Density and pressure of the medium fluctuate periodically due to these wave propagations.

Shear wave is another kind of wave which propagates from ultrasound and it is called transverse wave. These types of waves are perpendicular to the direction of the wave propagation. **Fig 10** shows the two different modes of ultrasound wave propagation; those are longitudinal and transverse.

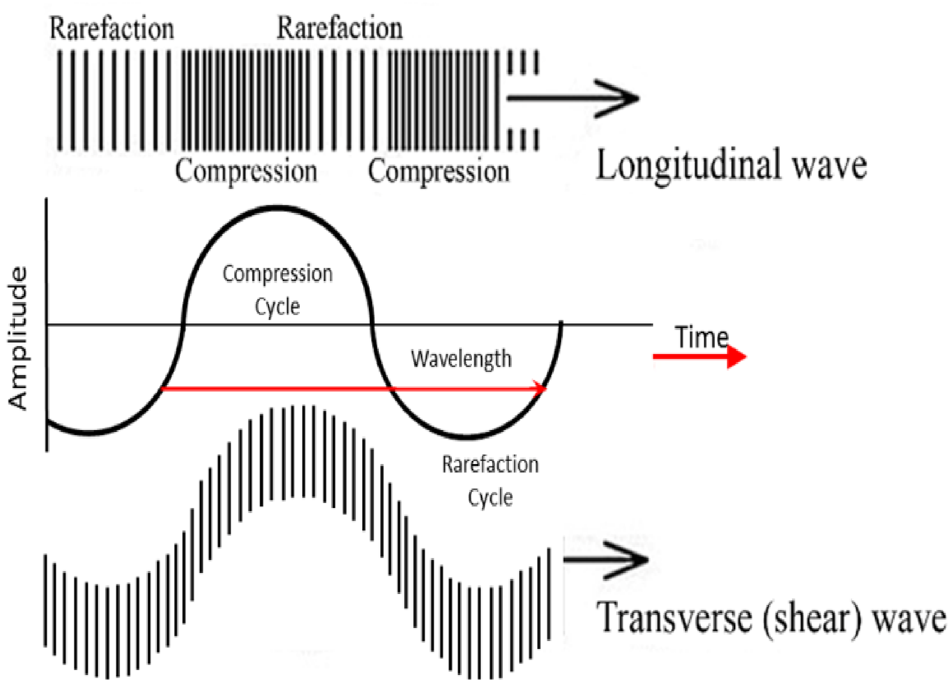


**Fig 10**. Longitudinal and shear wave behavior [7].

## 2.5 Analysis of ultrasonic techniques on carbon fiber sandwich material

The inspection of the object in ultrasonic NDT consists of several ultrasonic methods. The selection of the best possible method depends on different parameters of the specimen like its dimension, position, properties, structure and the material conditions and the limitations of the inspection, as each technique has its own advantages and limitations [22].

There are different possible techniques to investigate defects on carbon fiber sandwich panel, but every technique has limitations to the investigation. The immersion and air-coupled method investigation give C-scan results, these results help to obtain the size of the defect precisely and to estimate the depth of the defect. The ultrasonic phased arrays provide A and B scan results with better understanding, The B-scan gives the depth of defect on specimen precisely.

For the inspection of carbon fiber sandwich material suitable ultrasonic techniques are analyzed to investigate the sample to achieve the goal of the thesis.

### 2.5.1 Air coupled method

Air-coupled method is one of the non-destructive ultrasound techniques that helps in testing the properties of the material such as Young's modulus, density and also allows testing of homogeneity and flaws. In this technique, the typical ultrasonic gel, water and air from the surrounding is used as the coupling medium between the specimen and transmitter or between specimen and receiver. Using air as coupling medium is of great advantage as it avoids the use of complex coupling techniques like other ultrasonic methods in NDT. This method is also efficient as it requires only few centimeters distance from the object, it is also advantageous that measurement can be carried out from only one side.

The air-coupled technique with through transmission method can be used for investigation of carbon fiber sandwich material but these types of investigations need to access one side of the sample and it can obtain only C-scan view precisely. There is another method to investigate carbon fiber sandwich material with one side access which is a pitch-catch method. The impressive advantage of this method helps to obtain the results with one side access on field investigation [9].

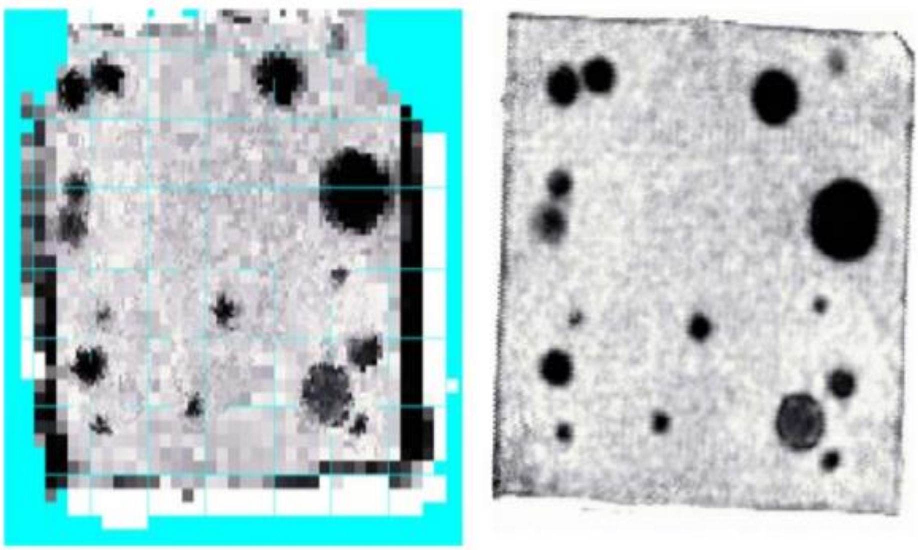

**Fig 11**. C-scan view of air-coupled investigation [9].

The inspection of the ultrasonic air-coupled method on solid materials is inefficient as energy is transferred from air to solid. The air and carbon fiber material acoustic impedance ratio are 1:10000. **Fig 11** shows the c-scan view of the air-coupled investigation.

The plane view of the C-scan results helps to estimate the size of the defect, but the depth is hard to estimate. Thus, the ultrasonic pulse-echo results give the size and depth of the defect accurately.

### 2.5.2 Through transmission

The sound through the material passes only once in through transmission technique and hence this technique is basically used for materials which possess high attenuation. For the sample to be inspected in this technique needs access to both the sides of the component and also no detailed information about the depth of the defect on provided sample. **Fig 12** shows the principle of through transmission method [23].

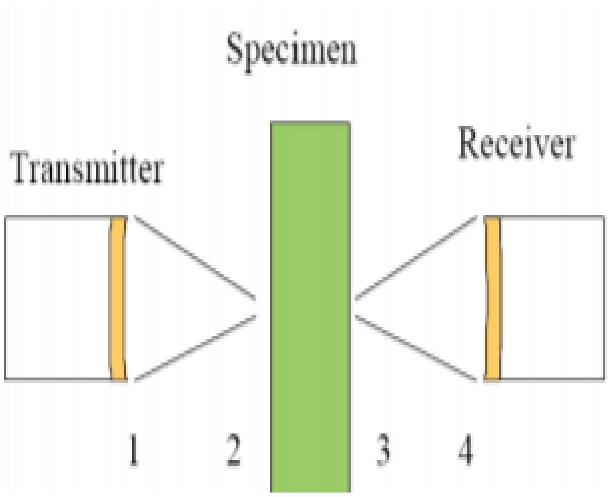


**Fig 12**. through transmission configuration [23].

**Fig 13** shows the on-field through transmission technique. The main disadvantage of this method is that it needs access to both side of inspection area.

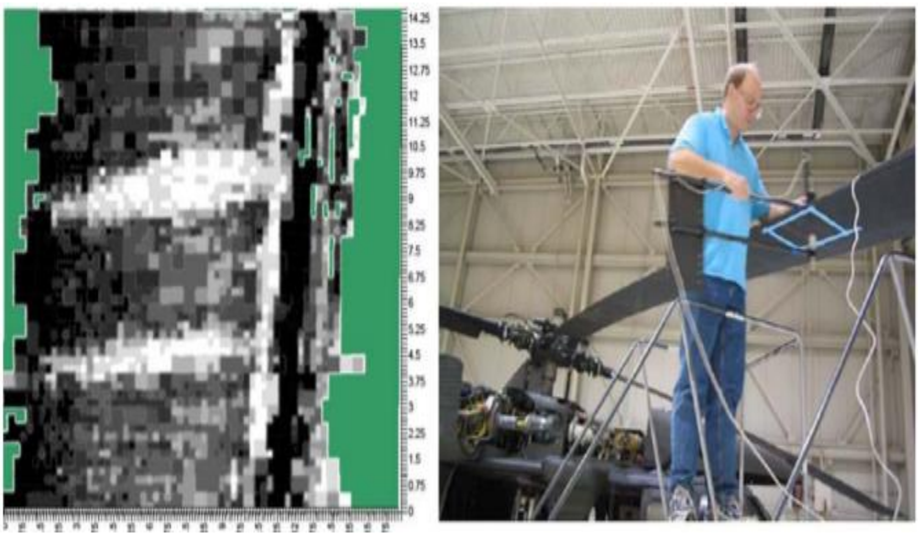

**Fig 13**. On field air-coupled through transmission investigation [9].

### 2.5.3 Pulse-echo Phased Array

Pulse-echo method is one of the NDT technique which uses ultrasound waves to find defects in the materials. The system consists of a transmitter and a receiver. The transmitter generates a pulsed ultrasound wave that is reflected by an inhomogeneity such as the defects in the material or the back wall of the object and is received by the receiver. Only one side of the component's access is required and the complete information on the exact position of the defect and also its depth is provided.

As in the conventional method of single element transducer that gives the disadvantage of less coverage area of inspection. Hence, increasing the number of elements in the transducer, large area can be covered for inspection, they can be configured electronically, the focusing can be optimized and also the ultrasonic beam can be oriented.

## 2.6 Evaluation of different types of transducers

The probe is an electronic device, it converts the electrical signal into mechanical signal. There are different types of ultrasonic transducers,

- Dual element transducer
- Angle beam transducer
- Delay line transducer
- Single element contact transducer
- Phased array transducer

*Dual element transducer* – these types of transducers are made of two elements which accommodates in single transducer housing. One element is to transmit and another one is to receive the signal from reflection. Dual element transducers are good for the surface flaws and useful for the thickness measurement of the thin test pieces. **Fig 14** shows the dual element transducer set-up and transducer composition [24].

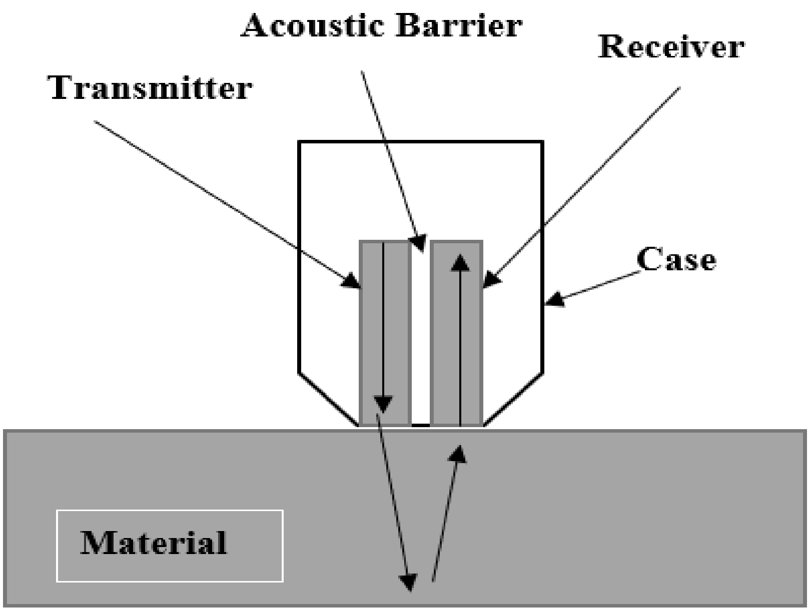


**Fig 14**. Dual element transducer set-up [20].

*Delay line transducer* – The function of the delay line transducer is providing a time delay between generation of sound energy and receiving sound energy. These types of transducers are mostly used for thickness measurement for thin materials, delamination defects in composite materials and high-temperature applications.

*Angle beam transducer* – In general angle beam transducers are used to produce refracted shear sound waves to propagate in certain angle into the test piece. These transducers help in finding the flaws in different positions inside the specimen and welded defects are estimated using angle beam transducer. **Fig 15** shows the angle beam transducer set-up and transducer composition.

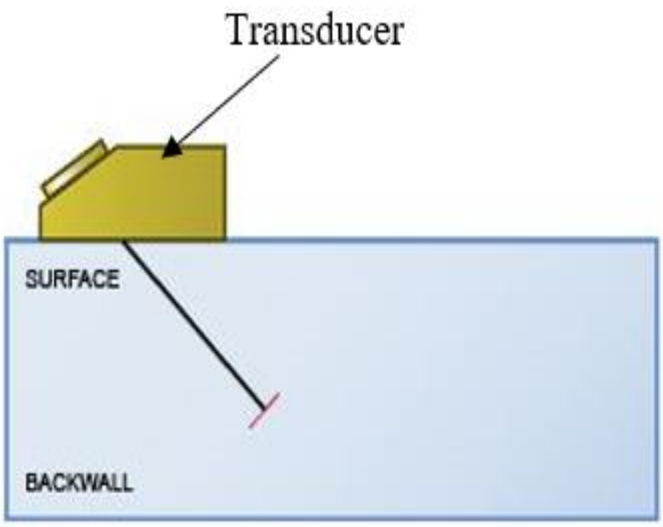


**Fig 15**. Angle beam transducer set-up.

*Single element contact transducer* – A single transducer consists of single crystal element housed in the casing. The single crystal performs both transmission and reception of sound energy. It is normal for the single element transducer to be provided with a delay-line to enable accuracy estimations on more thin materials. Transducers are chosen by the frequency and size of the crystal. The type of material and expected thickness range selects the frequency of the fitting transducer. It have single piezo element crystal accommodated in transducer case and the transducer transmits and receives the reflected sound energy [25].

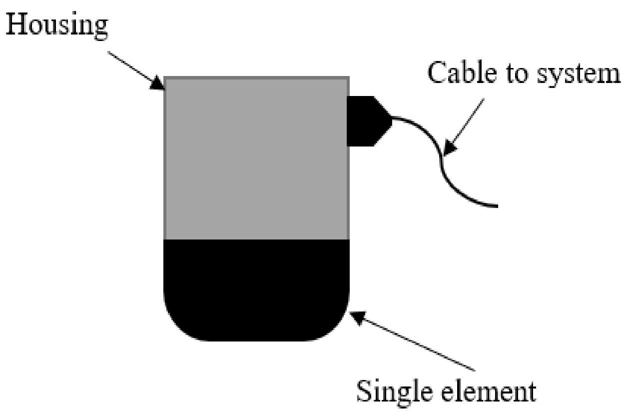


**Fig 16**. The single element transducer set-up.

Mainly single element transducer consists of four components, piezo element, matching layer, backing layer, housing shield and cable. The crystal size of the element varies with specimen access, size, thickness and surface finish [26]. table.4 illustrates the transducer specifications; the frequency increases both piezo element and diameter decreases. The composition of single element transducer is shown in **Fig 16**.

Table 4. Frequency range and piezo element size.

| **S. No** | **Frequency (MHz)** | **Piezo element (inch)** | **Diameter (mm)** |
|---|---|---|---|
| 1. | 0.5 | 1 | 25 |
| 2. | 2.25 | 0.5 | 13 |
| 3. | 5 | 0.25 | 6 |
| 4. | 10 | 0.125 | 3 |

*Phased Array transducer* - The Phased array has a unique quality to use all the elements simultaneously while applying different delays to each element. The large number of elements increases the large area, focusing and steering capability. The design of transducer includes crystal shape, whole aperture, grid and gap of elements and dimension of the elements [27]. The focal spot size is dependent on the focal length (F), wavelength (γ) and active aperture (A) of probe. The probe parameters are shown in the table 5.

Near field = A2/4λ;

Focal spot size of the probe = Fλ/A

Table 5. parameters of the probe.

| **S.no** | **Probe** | |
|---|---|---|
| 1. | Mode | Transmission/Reception |
| 2. | Type | Contact |
| 3. | Crystal | Linear Phased array |
| 4. | Wedge | Yes |
| 5. | Central Frequency | 3.5/5 MHz |

The series of elements together form the waves with different time delays. **Fig 1**7 shows the linear array transducer elements pattern. The elements are placed together in a row in linear array transducer. The series of elements steer the sound waves with particular time delays. Due to the time delay, the elements create a concave shape wave pattern and it helps better sensitivity to defect the flaws on the test piece.

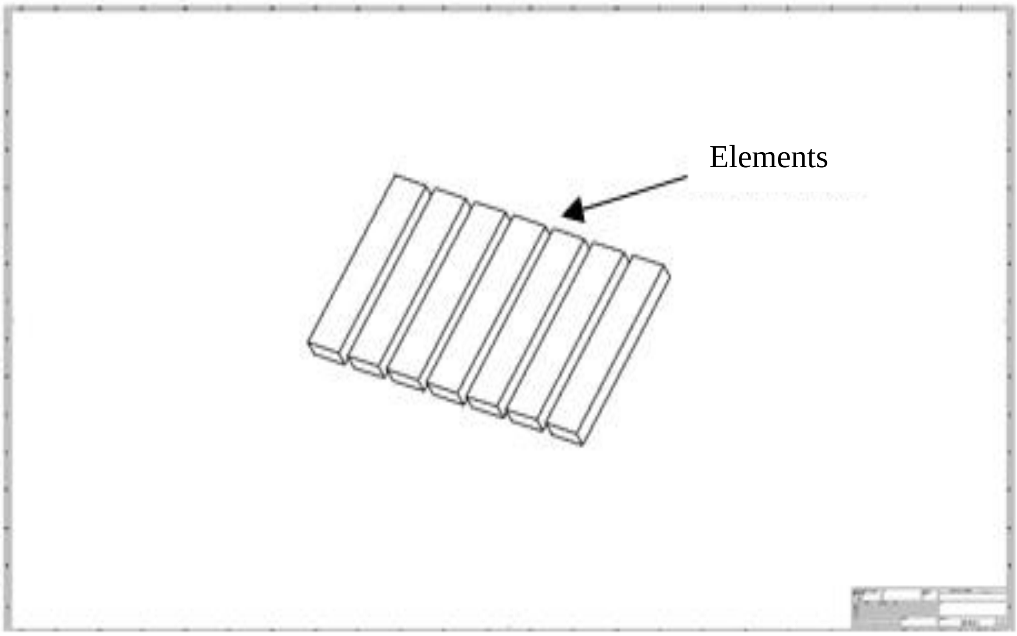


**Fig 17**. Linear array transducer elements.

Basically, the wedges are used for coupling the sound energy. The thin material inspection is the most difficult thing for the ultrasound. Because the ultrasound energy has to travel some distance to capture the defect. Otherwise, it causes multiple reflections and con not estimate the flaws. It also helps to avoid the scratches to the surface of the transducer from the rough surface. The wedges are used for shear waves and longitudinal waves. The sound energy is propagated to the specimen and when the velocity of the sound energy varies it is refracted back in a certain angle according to Snell's law.

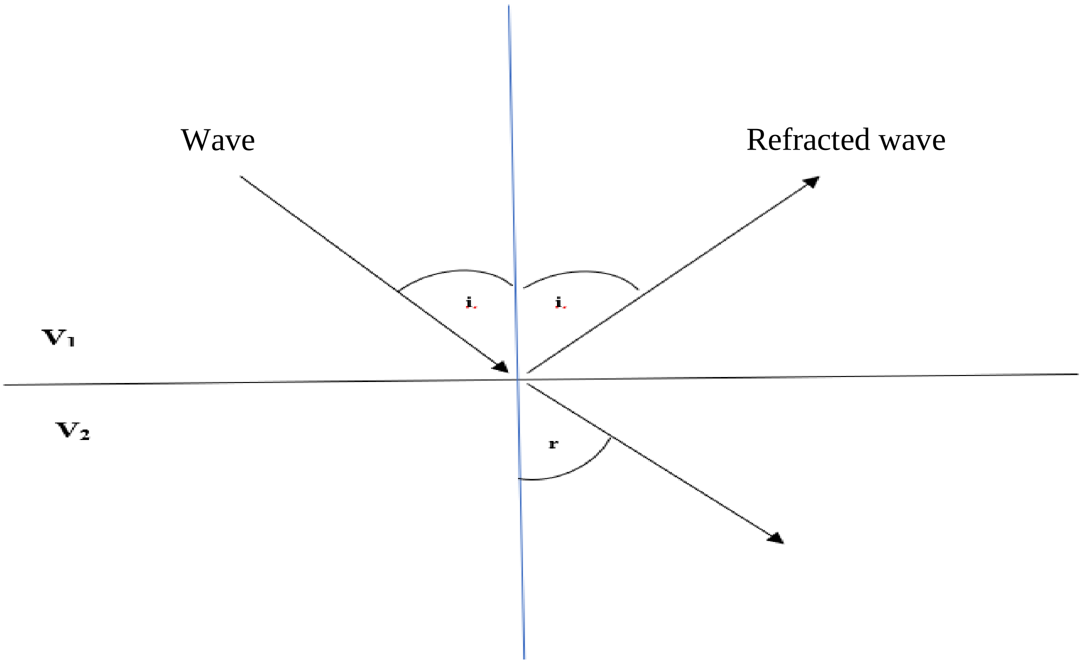


**Fig 18**. Ultrasonic wave diffraction due to velocity change [21].

**Fig 18** shows the ultrasound wave diffraction due to velocity change and the wave character. It is defined as; the excited sound wave changes the direction of angle due to velocity change whic is called Snell's law.

$$\frac{\sin i}{\sin r} = \frac{V_1}{V_2} \quad (5)$$

Where "i" is the incidence angle;

"r" is the refracted angle

## 2.7 Conclusion

The various aspects of non-destructive ultrasonic techniques on carbon fiber honeycomb sandwich material investigations were studied. The investigation on CFSM is one of the major concerns to identify the delamination defects. The delamination between carbon fiber skin and honeycomb Nomex sheet leads to damage the aircraft control surfaces like rudder, ailerons and spoilers. The air-coupled and immersion methods give slightly similar results i.e. C-scan. These two methods are time consuming techniques and it's difficult to inspect on field investigations. The ultrasonic investigations with single element transducer are very difficult to identify the defect on CFSM. Ultrasonic inspection with phased array is one of the essential options to carry out the inspection. The main advantage of using phased array is that is saves the inspection time and gives the large area coverage. The speed of ultrasonic pulse-echo inspection with phased array compare to air-couple and immersion is 5 times faster.

## 3. CIVA computer modeling and analysis on carbon fiber material

In the field of NDT, modeling is an important aspect to analyze and characterize the material integrity. CIVA computer software helps to develop and optimize the NDT simulation technologies. The position, geometry of defects and identification of defects can be obtained using CIVA. In order to analyze in software, the planar composite material was designed, and the sample was modeled with single ply laminated carbon fiber skin and aramid material as core. In the modeling, two types of composite materials have been constructed.

### 3.1 CIVA simulation set-up

The first model was designed with carbon fiber skin and aramid material. This model is used to analyze the carbon fiber material with a defect placed at different positions from the skin to core. **Fig 19** shows the simulation set-up in CIVA computational software [28].

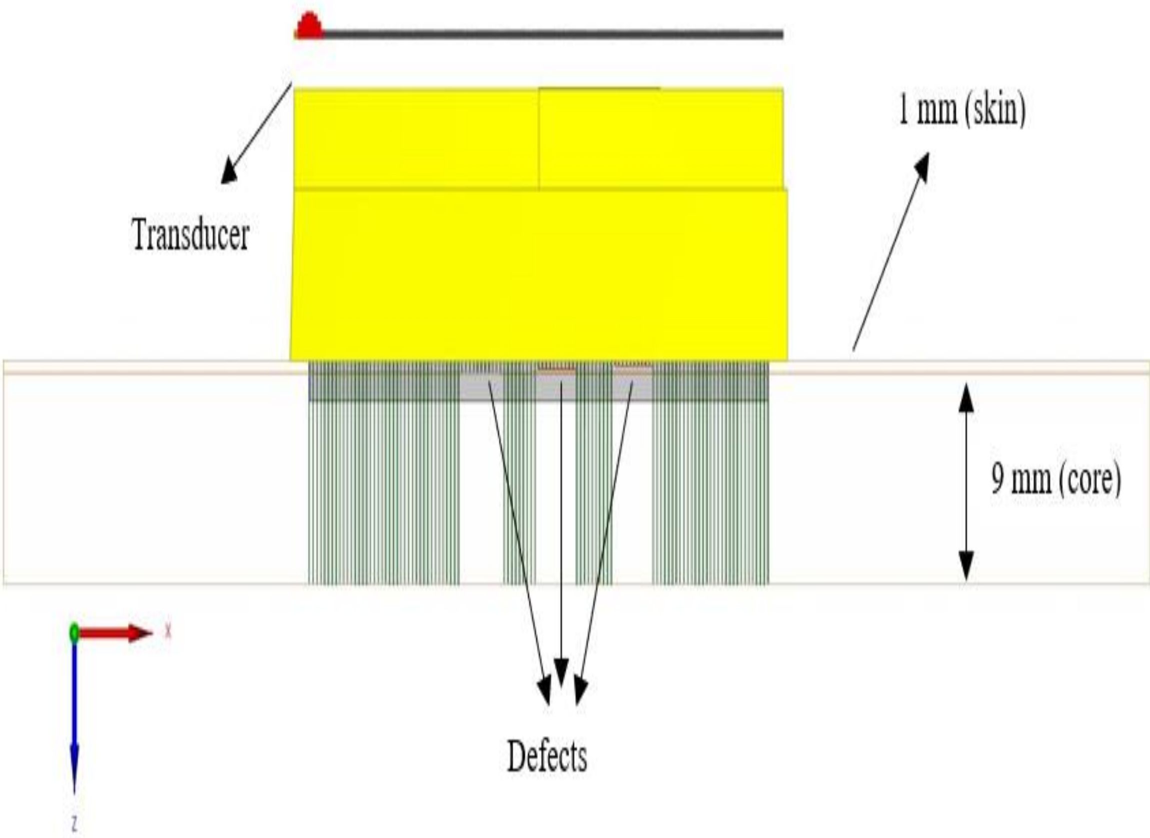


**Fig 19**. The simulation set-up on carbon fiber skin and core.

The second sample was designed with two skin materials with one aramid core. The material constructed as two skins are attached on both sides of the core material. Three artificial delamination defects are created between two layers with different size. **Fig 20** shows the set-up for the analysis of carbon fiber material.

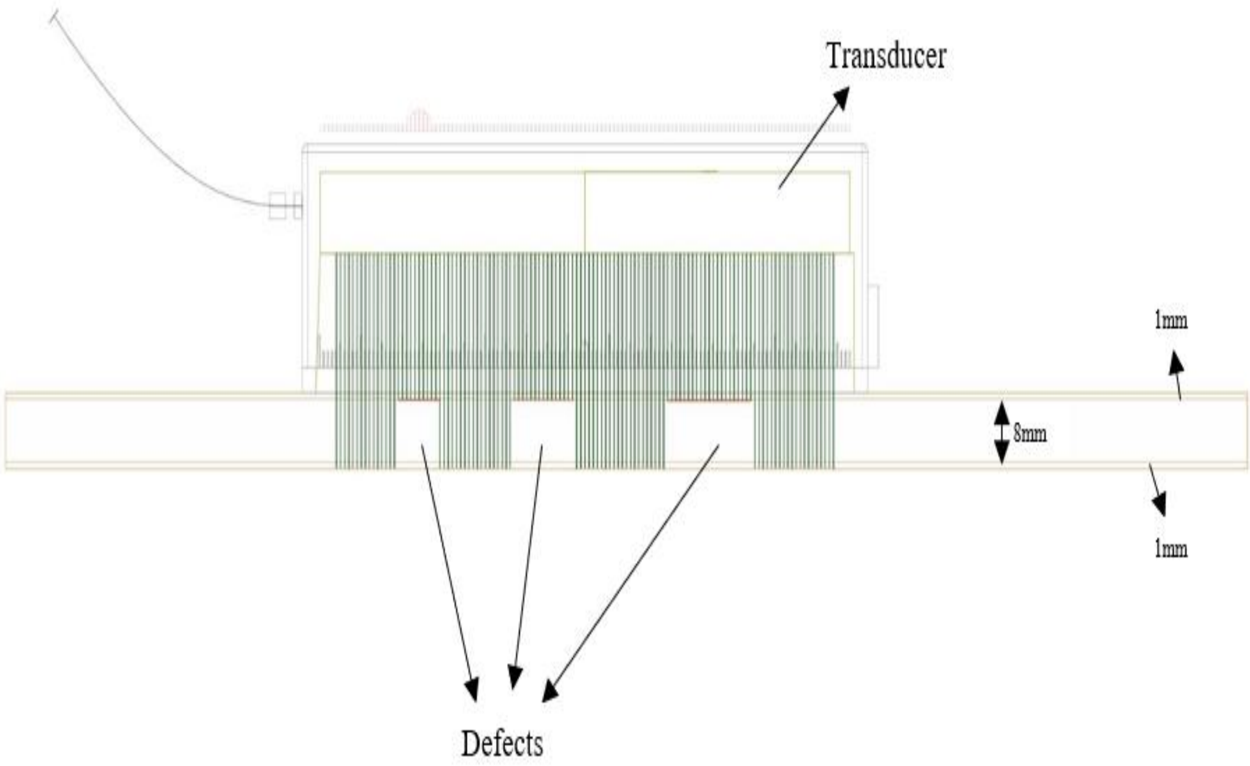


**Fig 20**. The simulation set-up of a sandwich structure with carbon fiber skin and core.

The inspection carried out on delamination between skin and core material. The general information about the specimen, table.6 the geometry and size of the material.

Table 6. Specimen parameters.

| **S.no** | **Specimen** | |
|---|---|---|
| 1. | Geometry type | Planar |
| 2. | Height | 28.5 mm |
| 3. | Length | 300 mm |
| 4. | Width | 200 mm |

The planar multilayer composite material has been designed. The thickness of single-ply composite layer is 1.5mm and it is made of carbon fiber epoxy, the fiber density is 60%, fiber diameter is 0.007mm and it is fully homogenized. The second layer is core material, the thickness of the core material is 27mm and it made of aramid epoxy. It is also fully homogenized [29].

Generalized Hook's law relates stress (σ) to strain (ε):

$$\sigma_{ij} = C_{ij}.\varepsilon_{ij} \qquad (6)$$

$$\varepsilon_{j} = S_{ij}.\sigma_{ij} \qquad (7)$$

Where,

i,j - 1 to 6,

$C_{ij}$ = Stiffness components,

$S_{ij}$ = Compliance components.

The inverse of compliance matrix S is stiffness matrix C and vice versa:

$S = C^{-1}$

$C = S^{-1}$

The material which changes the properties according to direction is called orthotropic materials. There are nine elastic constants in orthotropic materials. In nine engineering elastic constants include three young's modulus, three poisons ratio and three shear moduli/modulus. The elastic properties which are obtained have been presented clearly in the matrix.

For an orthotropic material, the compliance matrix components in terms of the engineering constants are:

$$S = \begin{bmatrix} \frac{1}{E_1} & -\frac{v_{21}}{E_2} & -\frac{v_{31}}{E_3} & 0 & 0 & 0 \\ -\frac{v_{12}}{E_1} & \frac{1}{E_2} & -\frac{v_{32}}{E_3} & 0 & 0 & 0 \\ -\frac{v_{13}}{E_1} & -\frac{v_{23}}{E_2} & \frac{1}{E_3} & 0 & 0 & 0 \\ 0 & 0 & 0 & \frac{1}{G_{23}} & 0 & 0 \\ 0 & 0 & 0 & 0 & \frac{1}{G_{13}} & 0 \\ 0 & 0 & 0 & 0 & 0 & \frac{1}{G_{12}} \end{bmatrix} \qquad (8)$$

The computer-generated stiffness matrix for single ply composite with engineering elastic constants has been presented.

$$S = \begin{bmatrix} 142.171 & 5.235 & 5.235 & 0 & 0 & 0 \\ 5.235 & 12.568 & 6.699 & 0 & 0 & 0 \\ 5.235 & 6.699 & 12.568 & 0 & 0 & 0 \\ 0 & 0 & 0 & 2.934 & 0 & 0 \\ 0 & 0 & 0 & 0 & 5.09 & 0 \\ 0 & 0 & 0 & 0 & 0 & 5.09 \end{bmatrix}$$

Table 7. The material properties CIVA specimen.

| S.no | Properties | | Single ply composite | Aramid epoxy |
|---|---|---|---|---|
| 1. | Young's modulus | $E_x$ (GPa) | 142.17 | 77 |
| | | $E_y = E_z$ (GPa) | 12.568 | 8 |
| 2. | Poisson's ratio | $V_{xy} = V_{xz}$ | 5.235 | 4 |
| | | $V_{yz}$ | 6.699 | 3.5 |
| 3. | Shear modulus | $G_{xy} = G_{xz}$ (GPa) | 5.09 | 2.5 |
| | | $G_{yz}$ (GPa) | 2.934 | 2 |
| 4. | Tensile Strength | $X_t$ (MPa) | 1717 | 1377 |
| | | $Y_t = Z_t$ (MPa) | 30 | 18 |
| 5. | Compression Strength | $X_c$ (MPa) | -1200 | -235 |
| | | $Y_c = Z_c$ (MPa) | -216 | -53 |
| 6. | Shear Strength | $S_{xy} = S_{yz} = S_{xz}$ (MPa) | 33 | 34 |

The core material is an aramid-epoxy and it is an orthotropic material. An orthotropic material is completely defined by nine independent elastic constants. The most common elastic constants are Young's modulus or elastic modules in three orthogonal directions $E_1$, $E_2$, $E_3$, Poisson's ratio $v_{12}$, $v_{21}$, $v_{31}$, $v_{32}$, $v_{13}$, $v_{23}$, shear modules $G_{12}$, $G_{23}$, $G_{31}$ in the 1-2, 2-3, 3-1 planes respectively. The stiffness matrix of orthotropic (core) material. The table 7 shows the material properties in CIVA computational software.

$$S = \begin{bmatrix} 77 & 4 & 4 & 0 & 0 & 0 \\ 4 & 8 & 3.5 & 0 & 0 & 0 \\ 4 & 3.5 & 8 & 0 & 0 & 0 \\ 0 & 0 & 0 & 2 & 0 & 0 \\ 0 & 0 & 0 & 0 & 2.5 & 0 \\ 0 & 0 & 0 & 0 & 0 & 2.5 \end{bmatrix}$$

**Fig 21** shows the simulation set-up in CIVA. The transducer wedge is used for the better propagation of ultrasonic wave into the specimen, the Plexiglas material is used as a wedge. The wedge dimensions are front length ($L_1$) = 64, back length ($L_2$) = 64, width ($L_3$) = 33, height ($L_4$) = 22.

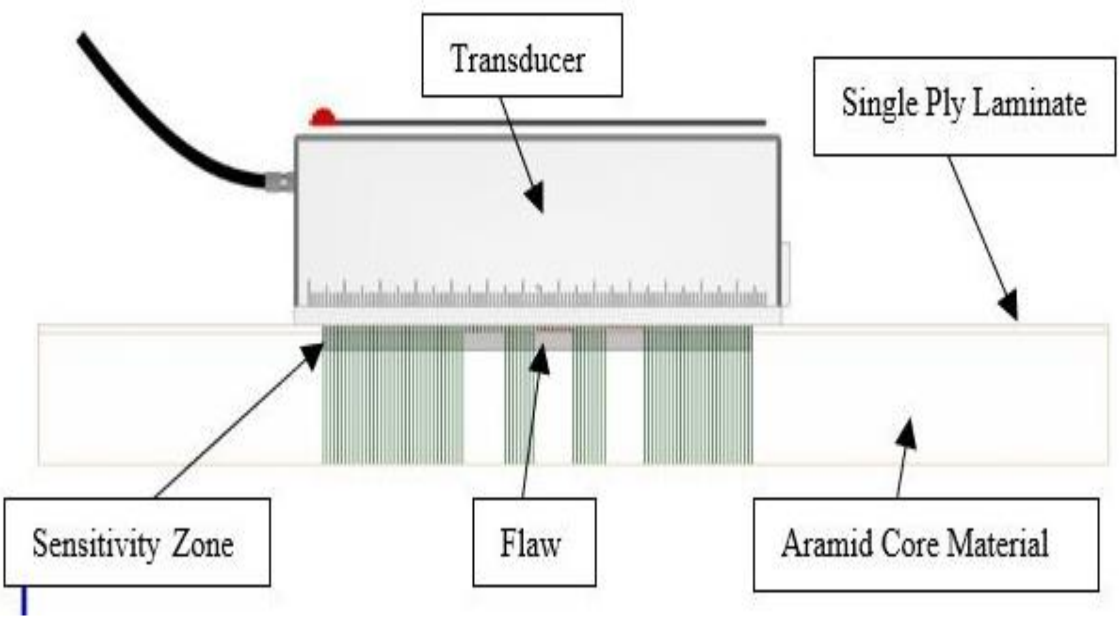


**Fig 21**. simulation setup on sample in CIVA.

Table 8. the transducer crystal shape parameters.

| **Transducer crystal parameters** | **3.5 MHz** | | | **5 MHz** | | |
|---|---|---|---|---|---|---|
| Incident dimension | 63.9 mm | | | 127.9 mm | | |
| Orthogonal dimension | 7 mm | | | 7 mm | | |
| Number of elements | 64 | | | 128 | | |
| Gap between elements | 0.1 mm | | | 0.1 mm | | |
| Active Aperture (mm) | 64 | | | 128 | | |
| Elevation | 7 | | | 7 | | |
| External Dimensions (mm) | L | W | H | L | W | H |
| | 66 | 19 | 25 | 130 | 21 | 35 |

The 3.5 and 5 MHz frequency have been used with the choice of the Gaussian signal, these signals are generating more cryptic signals than any other signals. The bandwidth of the signal is 65% and the phase is 90 degrees.

Table 8 shows the transducer crystal shape parameters for both 3.5 and 5 MHz frequency. The probability of defect detection is completely based on the transducer parameters.

The Ultrasonic phased array consists of a series of individual elements, each element radiates the signal with time delay. Elements are acoustically insulated from each other and pulsed with precalculated time delay.

By the influence of sound pressure, sound travels to the specimen. The more amount of pressure allows wave travel to the material. Acoustic impedance (Z) is defined as the product of the density (ρ) and acoustic velocity (C)

Therefore,

$$Z = \rho . C \qquad (9)$$

In order to calculate acoustic impedance to any material, the inspector has to realize material density and acoustic velocity of the material.

Appropriate delays introduced electrically during emission to generate a specific beam and it is generated by the Huygens principle. It is stats that, every point of wave-front act as origin of further wave-fronts, these wave-fronts are distributed into forward direction within the same speed as source wave.  During the reception, appropriate delays are introduced electronically.

Table 9. Computational settings in CIVA software.

| **S.no** | **Computational Settings** | |
|---|---|---|
| 1. | Function | Simple electronic scanning |
| 2. | Focusing (Emission/Reception) | Single point focusing |
| 3. | Model 2D/3D | 3D computing |
| 4. | Wave type | Longitudinal wave |
| 5. | Positioning | In the inspection plane |
| 6. | Type of coordinates | Cartesian X = 0; Y = 0; Z = 1.5 |

Signals satisfying the delay law shall be in phase and after summation a significant signal generates. Table 9 shows the computational settings of the Ultrasonic simulation in CIVA software.

The artificial rectangular delamination defects are created with the dimensions of 10 mm length and 10 mm in height. The defect is tilted into 90 degrees normal to the specimen surface. The position of the defect on length along x-axis from the surface. The gap between each defect is 25mm and it is along the normal direction of the surface of the specimen. **Fig 22** shows the placement of defects on the sample with respect to positions.

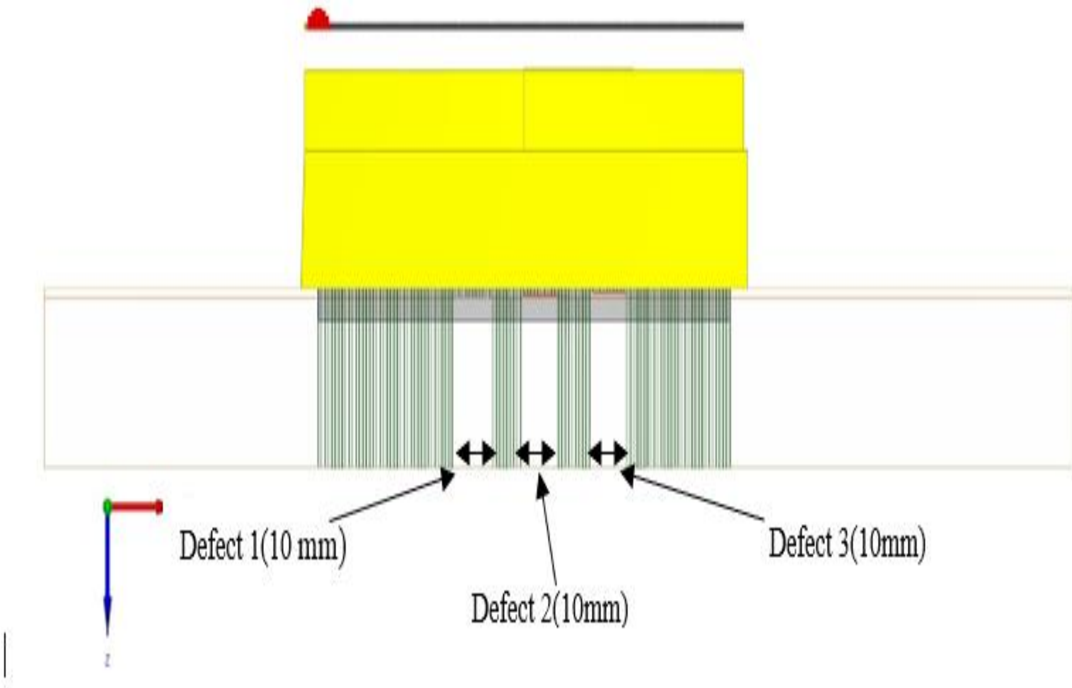


**Fig 22**. the placement of defects with different configuration.

**3.2 The CIVA computational results**

The ultrasonic inspection of carbon fiber sandwich material in the aeronautic industry motivates the development of dedicated simulation tools able to predict the propagation of ultrasonic wave to detect the abnormalities on complex materials. The delamination between the composite layers has been created artificially and the ultrasonic scan results are obtained in CIVA simulation software.

The direct control computation configuration is selected because the direct type computes contributions from flaws, with no skips on the specimen and direct skips from selected surfaces of the specimen. The longitudinal wave modes have been involved. The interactions of the wave with the specimen are a front interface, bottom and sides.

The sensitivity zone is enabled that concerns the defects and the depth direction of the sensitivity zone is along local normal. The 3D computation mode is enabled to get precise results. The field reflector interaction is plane wave approximation for the incident beam. In the accuracy field, the defect is one each and account for attenuation is activated. Attenuation is a natural consequence of signal transmission over long distances.

**Fig 23** shows the 3.5 Mhz E-scan view of ultrasonic phased array simulation. E-scan is a single focal law multiplexed across a group of elements for a constant angle beam stepped along the probe length. The three rectangular delamination defects are placed from single plate laminate surface to core interface. The defects are placed in different positions in terms of depth. The different position of depth used to obtain the results at different positions on sample. The depth of the defects are 0.5 mm, 1 mm, 1.5 mm respectively.

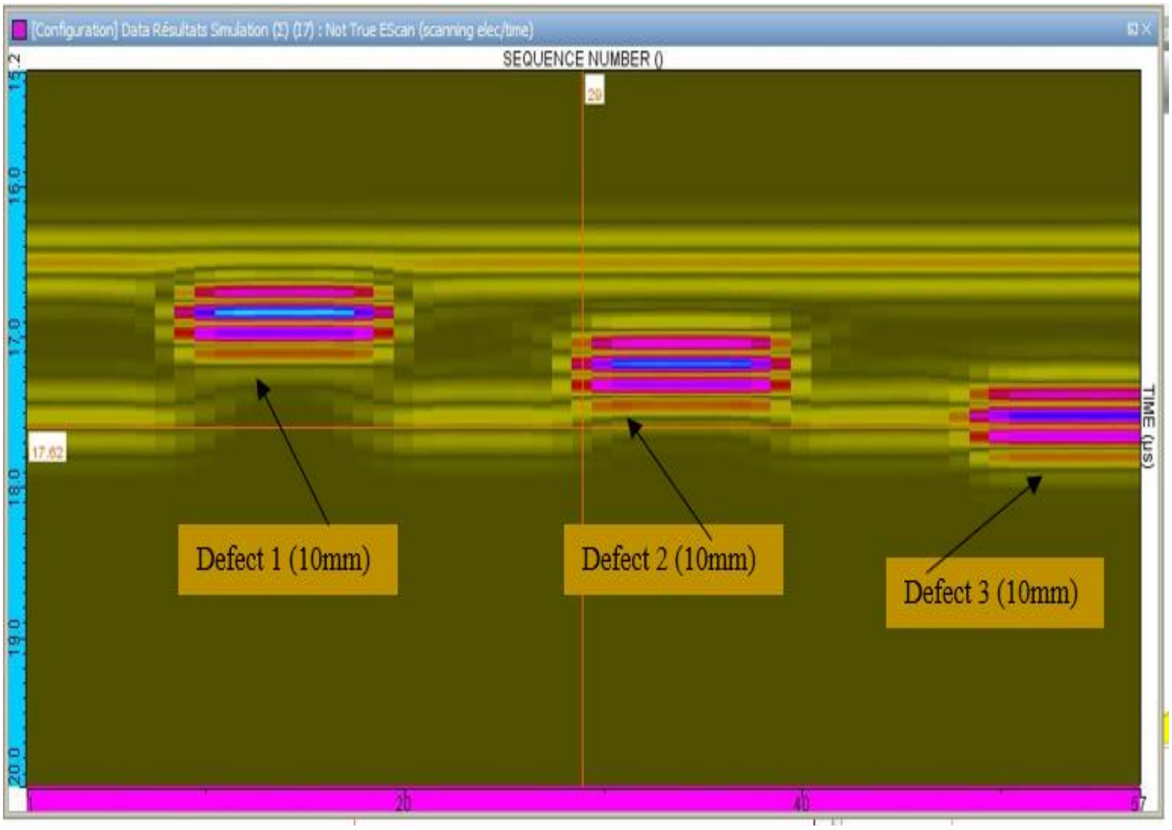


**Fig 23**. Scan view of identified defects with different depth using 3.5 MHz frequency.

The size of the defects was the same for all three and the depth has been changed from very near surface of the skin to interface of core material. The defects are analyzed with 3.5 frequency respectively. **Fig 24** shows the A-scan of the three defects at different positions with 3.5 MHz frequency. Each defect obtained are in different range of amplitute with respect to time.

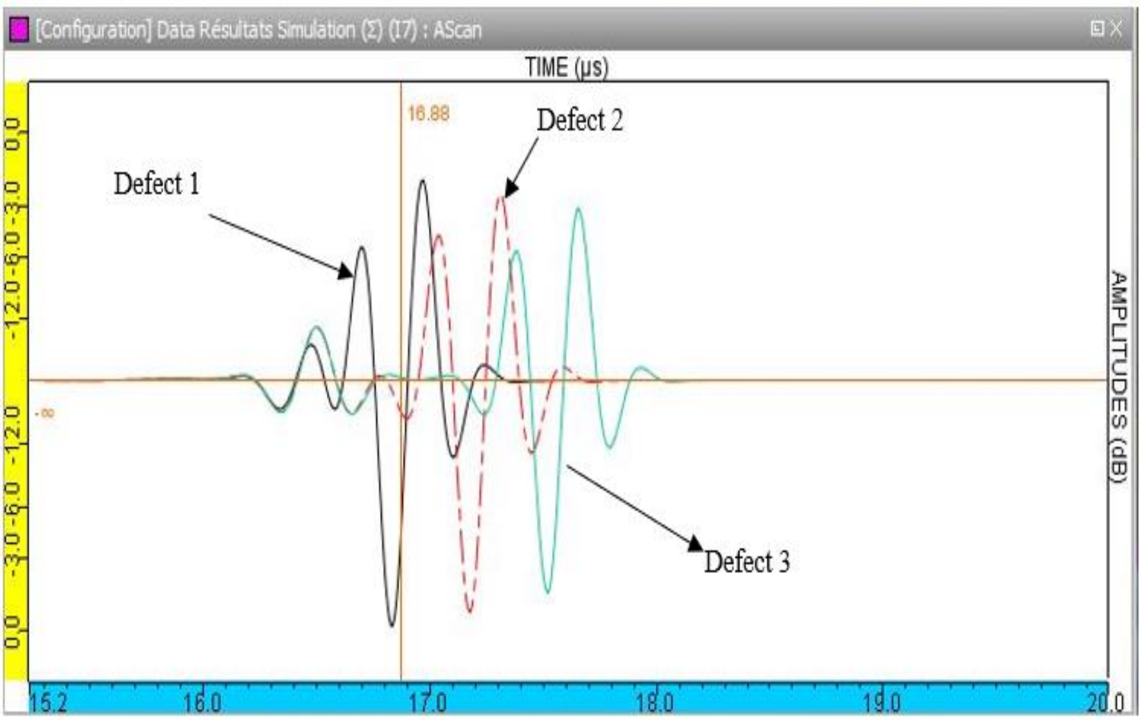


**Fig 24**. A- scan view of the three defects placed on sample analyzed with 3.5 MHz

The CIVA ultrasonic analysis carried out with same defect configuration but different frequency ranges are used to obtain the precise result. The placement and position of the defects remain same as above mentioned analysis. The same simulation set-up used with 5 MHz frequency to obtain the different analytical results. The 5MHz frequency gives much better results. **Fig 25** shows the position of the defects near the surface of the skin to interface of the skin and core.

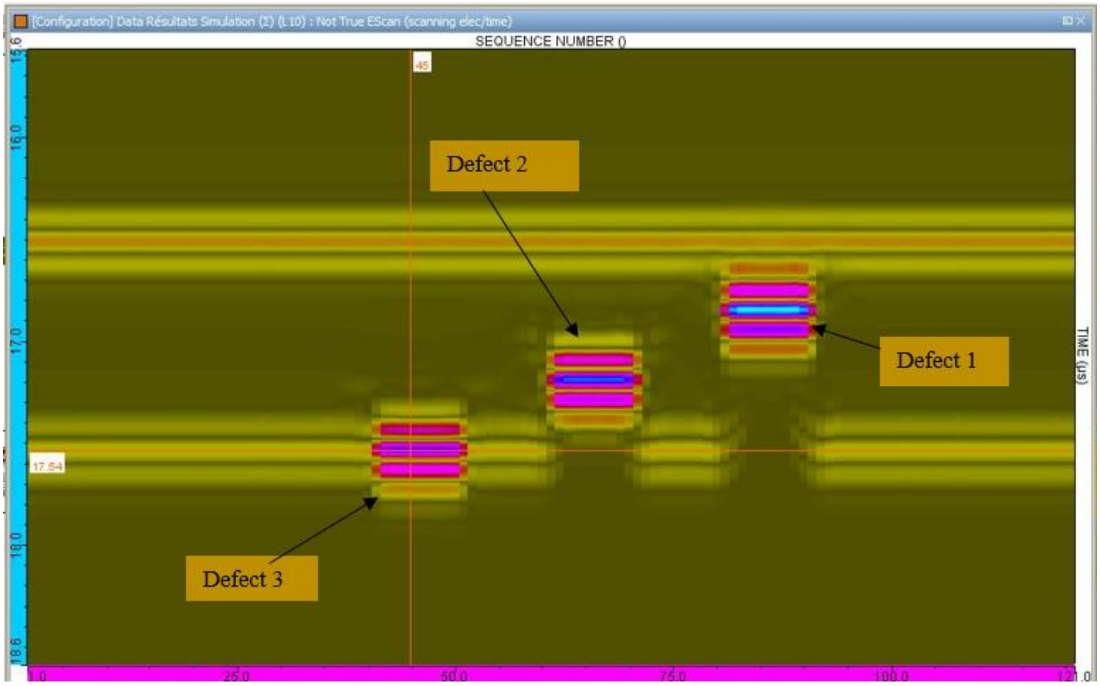


**Fig 25**. Scan view of identified defects with depth using 5 MHz frequency.

The comparison of both 3.5 MHz and 5 MHz results helps to understand the ultrasonic testing capability with linear phased array. The 3.5 MHz scan results are obtained with limited understanding about defect especially the 10 mm third defect placed at the interface of the skin and core.

The 5MHz scan results are obtained clearly with all three defects place on the model. Therefore, the difference in obtaining results with 3.5 and 5 MHz has been presented and discussed.

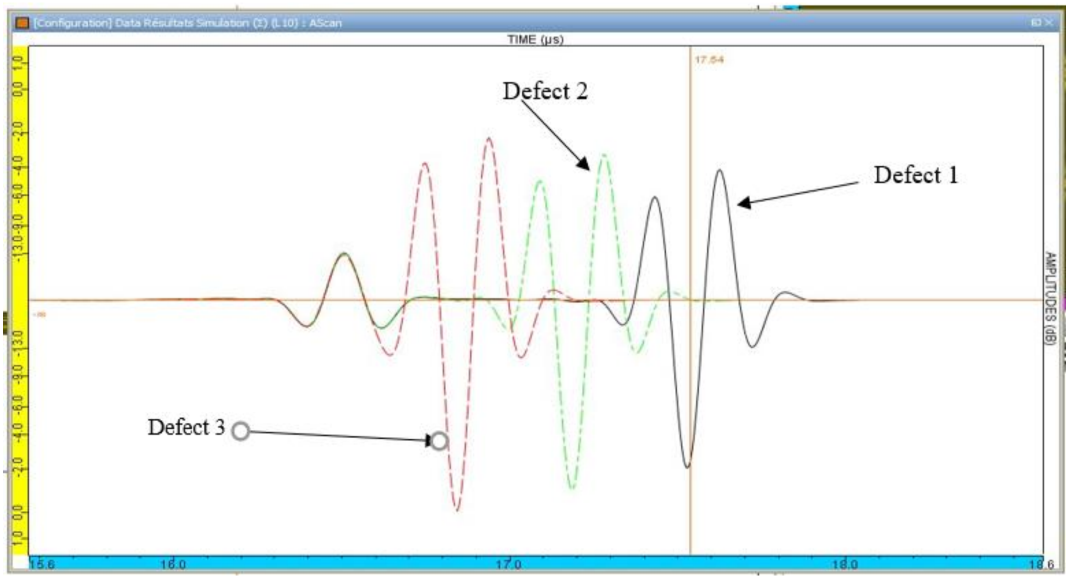

**Fig 26**. The A-scan view of the defects on sample with 5MHz frequency.

**Fig 26** shows the A-scan view of 5 MHz CIVA simulation results. The A-scan presents the amount of signal received with respect to time. The function of time on the horizontal axis and the amount of received amplitude on the vertical axis. The difference of amplitude with 5 MHz obtained results are presented and compared with three defects.

### 3.3 Carbon fiber sandwich modelling in CIVA

The carbon fiber sandwich model was designed with realistic parameters. The two-carbon fiber layer and one core material aramid epoxy made a stiff carbon fiber sandwich material. In order to increase the stiffness and bending properties, material designed with mentioned structure.

**Fig 27** shows that the core material is bounded by two thin carbon fiber (1 mm) material. The transducer placed on the carbon fiber skin and the contact medium set as water for better wave propagation. The defects are placed in between core and skin. The transducer elements in series can be seen on top of the transducer, the different size defects are underneath of the transducer.

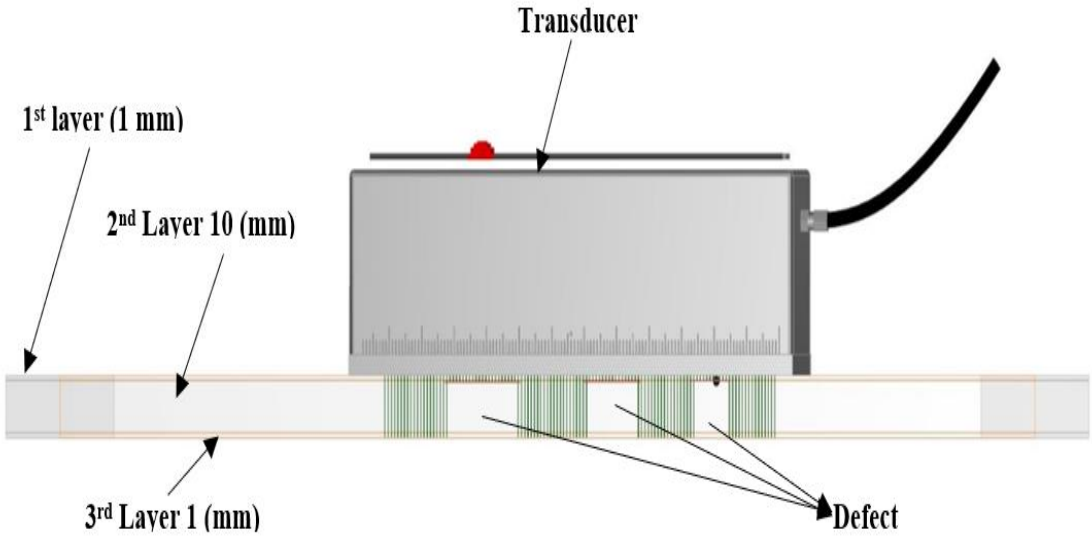


**Fig 27**. Composite model and analysis set-up.

The delamination type defects between the composite layers have been created artificially and the ultrasonic scan results are obtained in CIVA simulation software which uses phased array transducer at a frequency of 5MHz. The transducer uses 128 elements.

The longitudinal wave modes have been modeled. The sensitivity zone is enabled that concerns the defects and the depth direction of the sensitivity zone is along local normal. The defect depth and size have been obtained. In **Fig 28** shows the defects under the transducer.

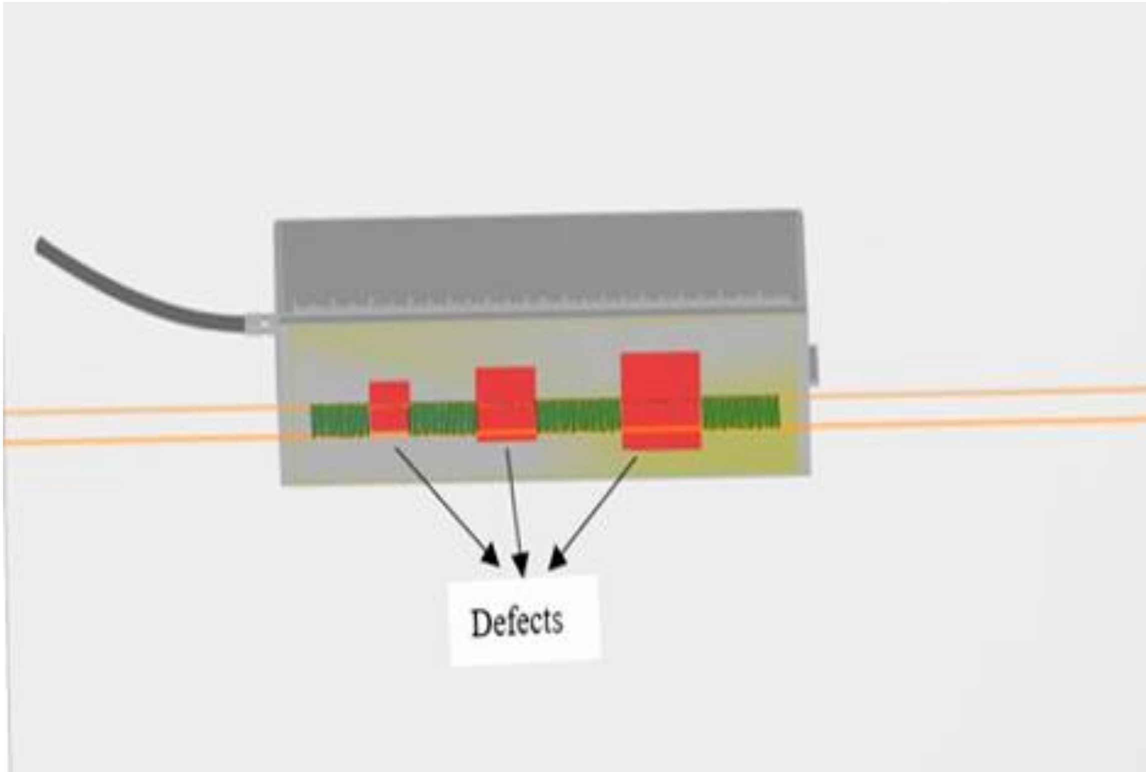


**Fig 28**. The placement of defects with different sizes.

The three different defects sizes are created and those are 10 mm, 15 mm and 20 mm respectively. The defects are placed in different depth position and the scan results are exposed clearly in scan view. The positions of the defects in terms of depth are 1.1 mm, 1.2 mm and 1.3 respectively. Table 10 shows the configuration of defects. The simulation was carried out with 5 MHz frequency on carbon fiber sandwich model.

Table 10. Defect parameters.

| **S.no** | **Defects** | **Type** | **Size** |
|---|---|---|---|
| 1. | Defect (1) | Rectangular | 10 X 10 |
| 2. | Defect (2) | Rectangular | 15 X15 |
| 3. | Defect (3) | Rectangular | 20 X 20 |

The second phase of analysis was carried out with 5MHz frequency and the defects were placed at different depths with different sizes. The scan results were obtained with the defect positions and depths precisely. The scan view of the CIVA computational software was also obtained.


**Fig 29**. Scan view of defects on model.

**Fig 29** shows the scan view of the defects on the designed model. The artificial rectangular defects are placed on the model. The defect detecting capability with linear array transducer was clear.

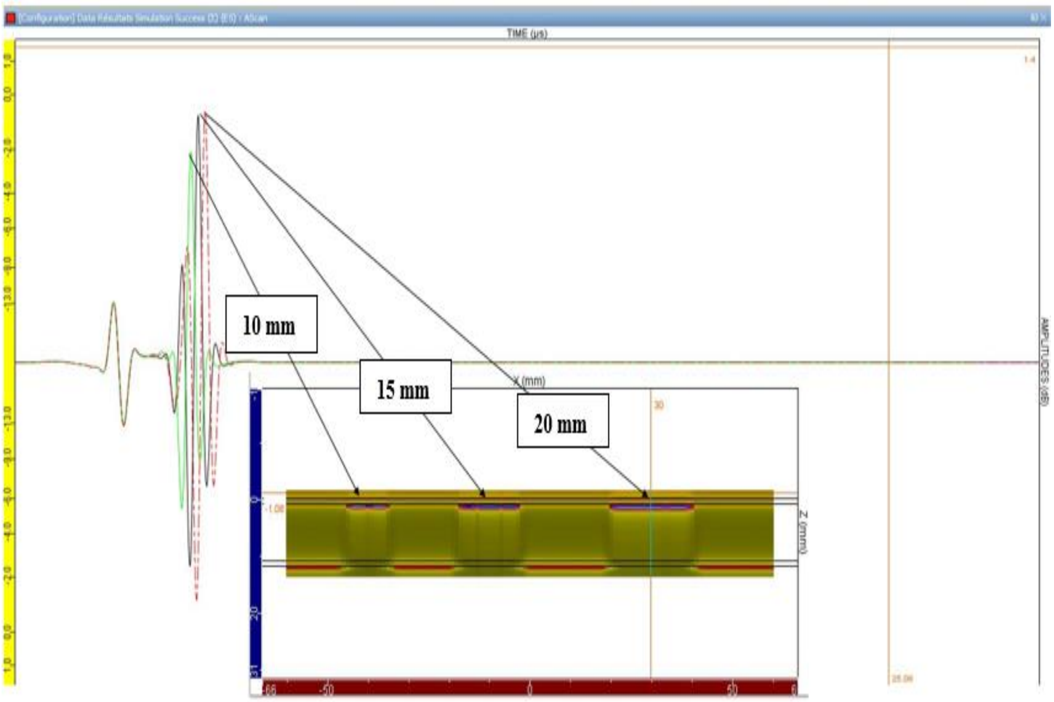


**Fig 30**. A- scan view of defects amplitude.

**Fig 30** shows the A-scan view of defects in the model and the plot was drawn with time versus amplitude. The defects identified with size 10mm, 15mm and 20mm respectively as shown in A-scan. The amplitude of the reflected signal with respect to each of these defects is also shown. The amplitude increases with the size of the defect as shown in the A-scan amplitude comparison.

### 3.4 CIVA conclusions

The artificial delamination defects have been created between the skin and honeycomb structure using CIVA software. The required parameters have been selected and applied to simulation settings. During the simulation, various parameters are noticed in order to see the variations in ultrasonic wave capability. The ultrasonic wave interaction with rectangular delamination defect between two layers have been obtained and interpreted. Simulation tools gathered in the CIVA platform provide an efficient solution to support NDE reliability.

The desired computational parameters are achieved which are to be applied to the experimental investigations. Due to 68 elements in 3.5 MHz frequency transducer, the steering capacity and area coverage is less. The 5 MHz frequency transducer has 128 elements, the steering capability and coverage area is more than 3.5 MHz transducers. The 5 MHz frequency is more suitable to identify the defects on carbon fiber sandwich material.  The results are achieved precisely using 5 MHz frequency transducer

## 4. CAD and FEM modeling

The finite element software is one of the numerical methods solving platform to perform simulation on engineering materials. It is one of the software to develop solutions on various engineering problems and material characterization. Finite element method gives the proper wave interaction with the material and the defects. Hence the FEM modeling was considered to view the wave propagation through the material and the interaction with the defect of the composite material.

The composite skin is modeled in solid works, the measurements of the plate are shown in **Fig 31**. The length of the composite skin is 10.41 mm and the width of the plate is 12 mm. In order to make a complete model, another skin has been modeled with same parameters. The model is designed in small scale measurements.

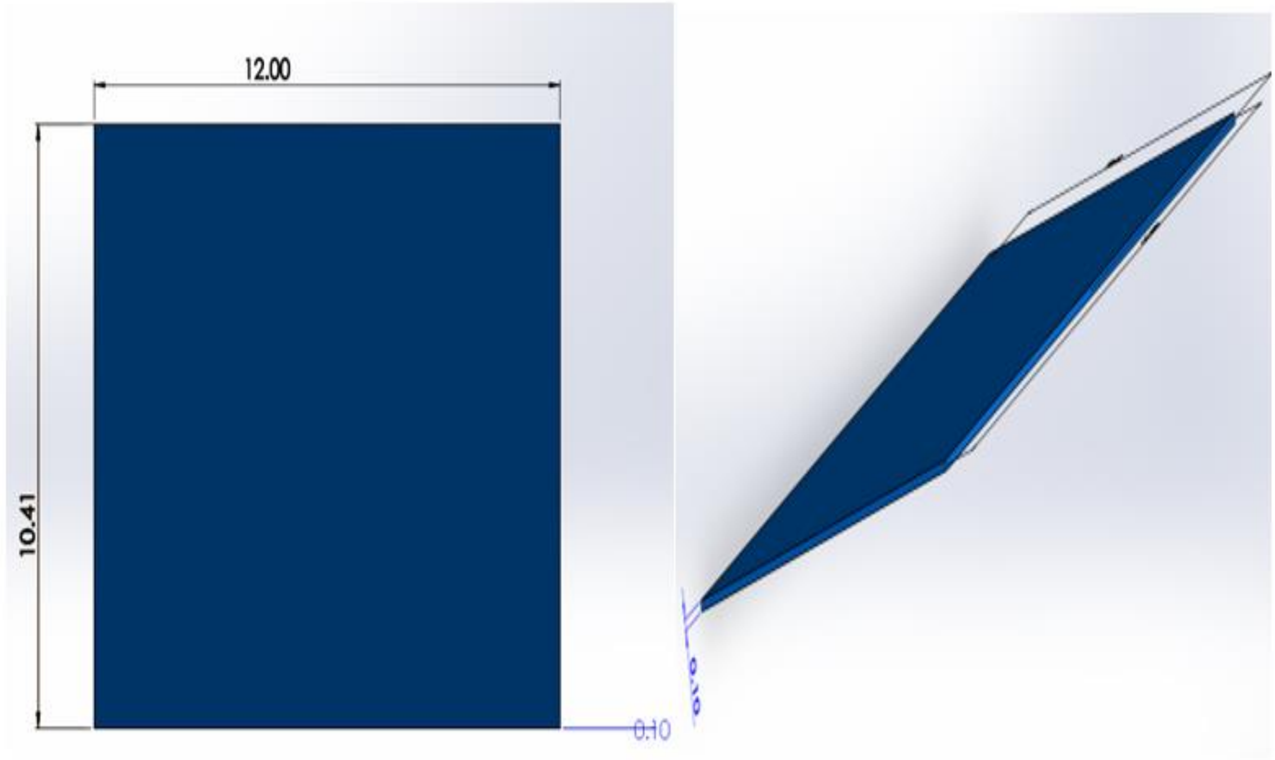


**Fig 31**. The geometry of composite skin.

The skin is an orthotropic material, the material contains nine engineering elastic constants such as Young's modulus $E_{1111}$, $E_{2222}$, $E_{3333}$, Poisson’s ratio $E_{1122}$, $E_{1133}$, $E_{2233}$ and Shear modulus $E_{1212}$, $E_{1313}$, $E_{2323}$ [19]. The density of carbon fiber sandwich material is 1570 kg/m$^3$.

$$\begin{bmatrix} E_{1111} & E_{1122} & E_{1133} & 0 & 0 & 0 \\ E_{1122} & E_{2222} & E_{2233} & 0 & 0 & 0 \\ E_{1133} & E_{2233} & E_{3333} & 0 & 0 & 0 \\ 0 & 0 & 0 & E_{1212} & 0 & 0 \\ 0 & 0 & 0 & 0 & E_{1313} & 0 \\ 0 & 0 & 0 & 0 & 0 & E_{2323} \end{bmatrix} \quad (9)$$

$$\begin{bmatrix} 4.8135e+010 & 0.6544e+010 & 3.7535e+010 & 0 & 0 & 0 \\ 0.6544e+010 & 1.3393e+010 & 0.6544e+010 & 0 & 0 & 0 \\ 3.7535e+010 & 0.6544e+010 & 4.8135e+010 & 0 & 0 & 0 \\ 0 & 0 & 0 & 0.4331e+010 & 0 & 0 \\ 0 & 0 & 0 & 0 & 0.4331e+010 & 0 \\ 0 & 0 & 0 & 0 & 0 & 3.6416e+010 \end{bmatrix}$$

The thickness of the skin is 1 mm. The model is designed with small parameters, because the small-scale size model helps to run the calculations in a simple way. High specification computer required for large scale models.

The honeycomb structure is designed with hexagons. The structure is constructed by the six-sided shapes that are arranged together to form a hexagon. Each side of the honeycomb structure is 1.74 mm.

The distance between each of the two opposite sides is 3 mm. The linear pattern option is used in solid works to construct the honeycomb core material. There is no gap between any two-honeycomb hexagon structures. The honeycomb aramid fiber thickness is 0.05, and the core is designed as surfaces because its thickness should meet paper thickness.

The assembled model contains three individual parts, which are core material with honeycomb structure and two skins that attach on both sides of the core and each part is designed separately.

The core material is taken as surface in order to avoid the gap between two hexagons. The thickness of each skin is 1 mm and core material height are 10 mm. The overall height of the carbon fiber sandwich model is 11 mm. The assembled model is shown in **Fig 32**.

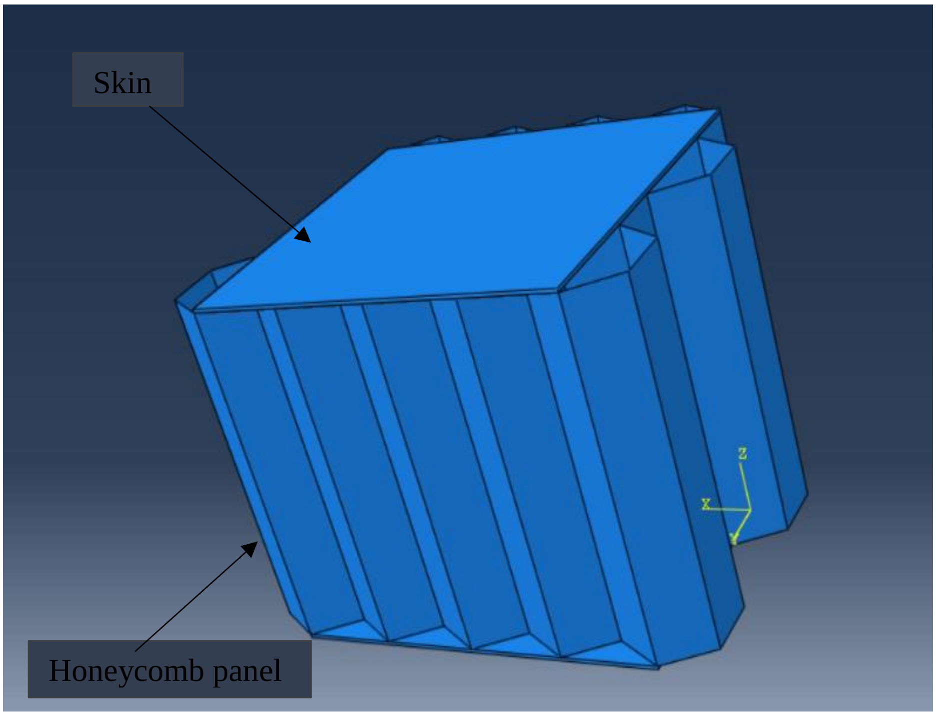


**Fig 32**. Carbon fiber honeycomb sample for FEM.

### 4.1 Finite element method modelling

The 2D model of carbon fiber reinforced plate with delamination type defects were prepared using Abaqus explicit finite element software. The thickness of the modeled plate was 1 mm. Investigations were carried-out using 5MHz frequency bulk ultrasonic waves in pulse-echo mode.

The two types of skin models are is designed for the finite element analysis. To demonstrate the ultrasound wave interaction on carbon fiber skin with defect and without defect. The defect was created with 0.02 mm size. The defect is placed in the middle part of the skin approximately 0.5 mm. The geometry of the defect is rectangular type defect. **Fig 33** shows the carbon fiber skin with the defect.

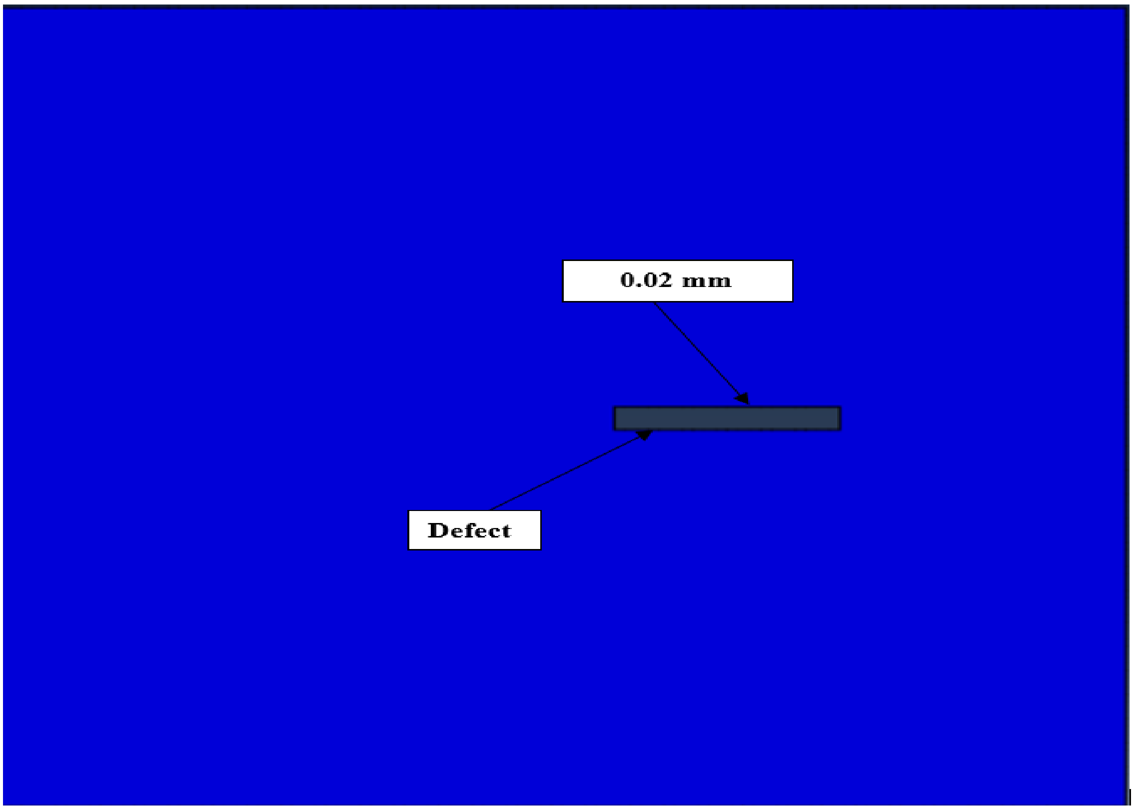


**Fig 33**. The carbon fiber skin with defect.

The ultrasonic waves excitation zone was placed on top of the plate at different positions-above defect free and defective zone. Let us assume that, the excitation zone acts as transducer to create and propagate the bulk wave on the skin material. The ultrasonic wave reflects at different positions detected and investigation of ultrasonic wave interaction with defects was carried out. The fine mesh was applied for the finite element analysis.

The mesh section is very important aspect in Abaqus software analysis, the initial stage of mesh is to assign the mesh attributes and set the mesh controls. In this module analyses need to specify the mesh density, element type and shape.

The mesh density is created by seeds along the model edges, the nodes are appearing on edge of the model. Two types of mesh controls are available in Abaqus/CAE; top-down and bottom-up. The top-down mesh to mesh is for 1D, 2D or 3D models. It is partially better topology, but it is difficult to generate a high-quality mesh for different shapes.

The bottom-up meshing is suitable for 2D model entities such as 2D element and geometric faces. It allows to be producing high-quality meshing properties. By using the tools in Abaqus/CAE optimized and refined the mesh using computational tools. The entire model is meshed, the 0.02 mm rectangular part is eliminated from the mesh. Then it is considered as defect on model. **Fig 34** shows the mesh model, excitation zone and defect.

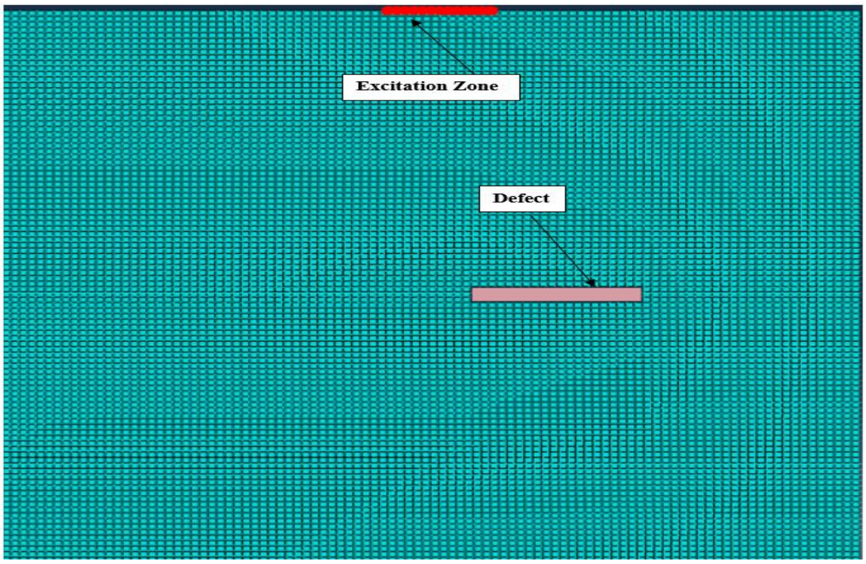


**Fig 34**. The Mesh attribution in Abaqus explicit.

The 5 MHz frequency is applied on the excitation zone and the load is applied to the bottom direction, because ultrasound wave must propagate to the bottom direction. The job is created and submitted for the simulation.

### 4.2 Finite element method results

**Fig 35** shows the ultrasonic wave propagation on carbon fiber skin in the absence of the defect.

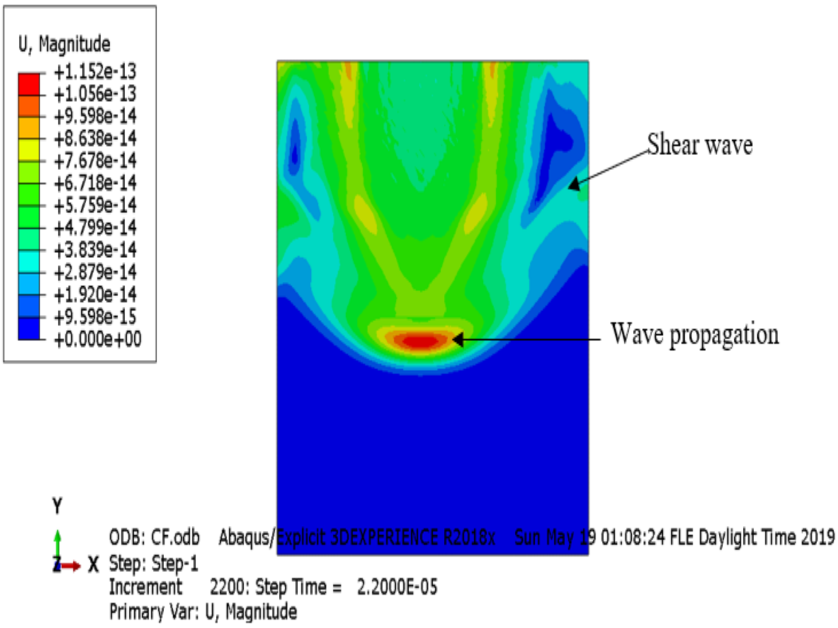


**Fig 35**. The wave propagation without defect.

The results are obtained on Abaqus/Explicit; the 20 steps procedures are done for the simulation. The increment for each step is 1400 and the step time is 1.1000E-05 (11 Nanoseconds). The primary variation is U magnitude and deformation variation is V deformation. The scale factor is +1.000e+00 and the step time starts from +0.000e+00 to +9.536e-14. For example, 10 Nanoseconds converted in milliseconds is 1e-5. The ultrasound bulk waves are propagated on carbon fiber skin. The bulkwave propagates towards down and the shear waves are propagated towards the boundaries of side walls. The nature of the wave is to propagate to the bottom layer and reflect back to the starting point with some loss of sound energy.

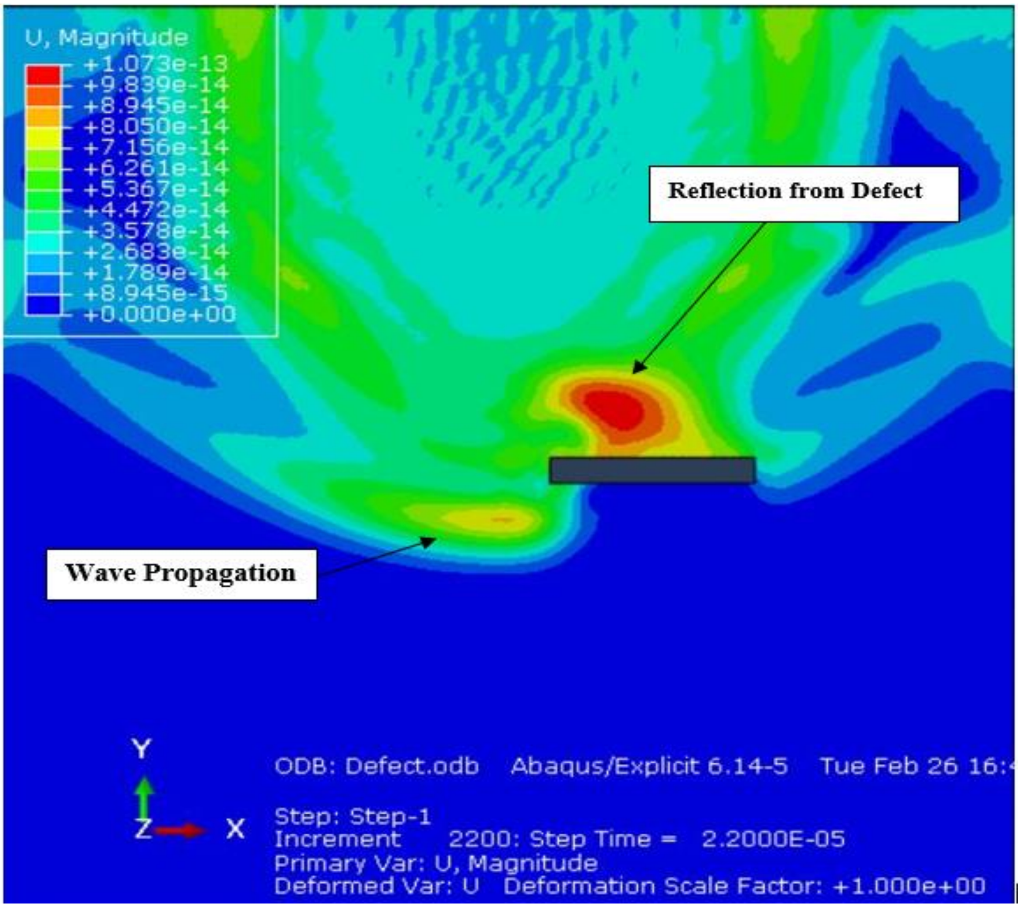


**Fig 36**. Wave propagation on defect area.

**Fig 36** shows the wave propagation on the defect. The excitation zone sets to meet the sound energy on the defect. The left-half wave is traveling on defect-free area and right half wave meets the defect on skin. Therefore, the right half wave is scattered with respect to the defect and reflected back to the origin. The left half wave has propagated to the bottom end and reflected back to the origin. The shear waves are scattered side walls of the model.

**Fig 37** shows the displacement of wave distribution in defect-free area. The wave propagates from the excitation zone with 5MHz frequency. The wave travels on the material with some loss of energy and the shear wave travels towards the side boundary of the sample.

Three path lines are drawn from the excitation zone to meet defect point, the displacement distribution of ultrasonic bulk wave versus defect meet point plot is drawn in the graphical map. The three path lines have different intensity of wave along with the direction of propagation.

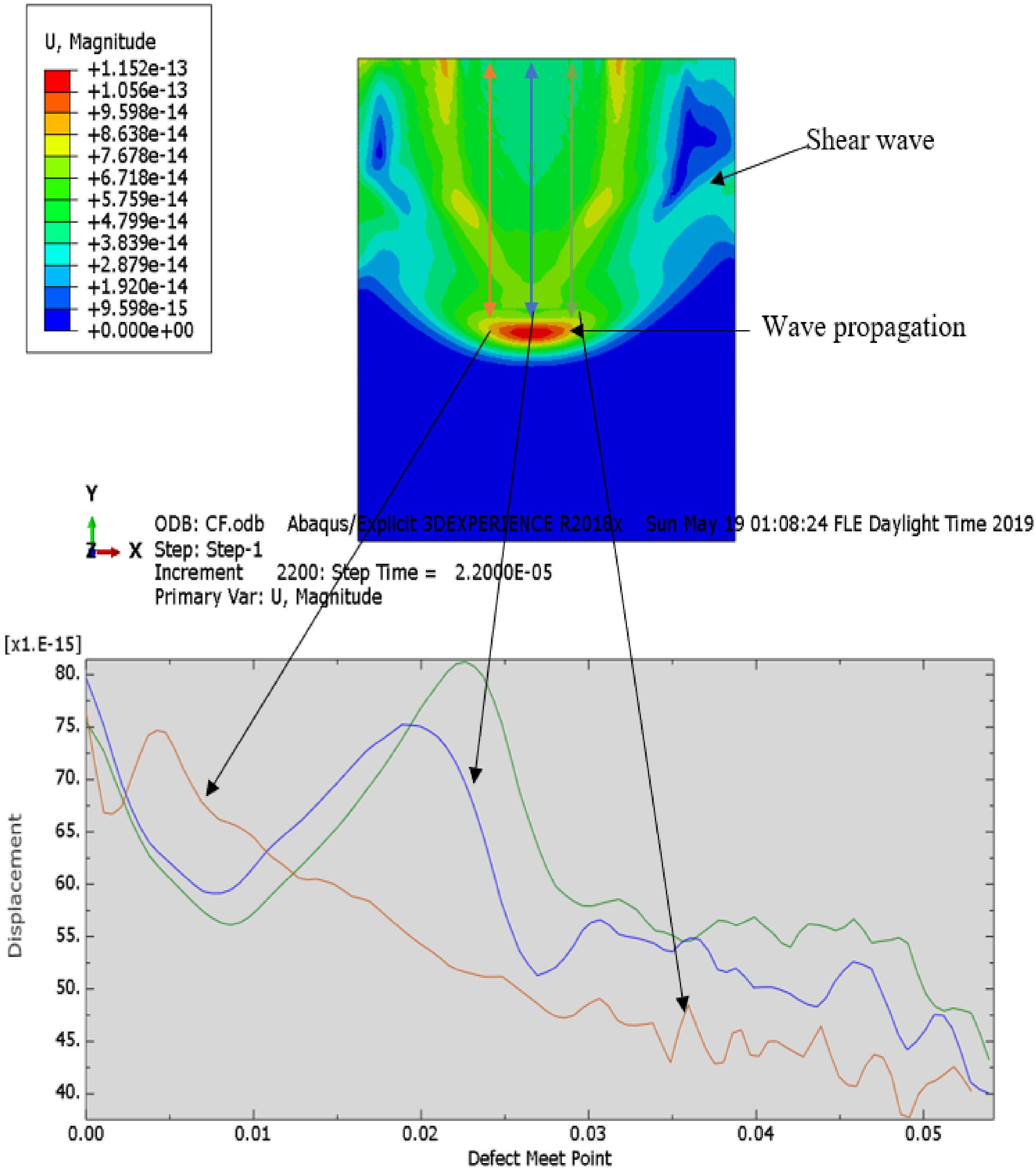


**Fig 37**. Displacement of wave distribution path on defect-free zone.

**Fig 38** shows the ultrasound wave distribution on defect placement zone. The graph plots with three paths between the excitation zone and defect zone. The shear waves are propagating towards the sides of the boundary and longitudinal wave travels toward the Y-direction on the Cartesian coordinates on the sample.

The first path line goes away from the defect and the displacement of wave shows the intensity of the wave. The second path line had met the defect with some energy and the displacement distribution is shown in the plot. The third path wave has high energy than path 1 and 2. The displacement distribution with defect meet point is shown in the plot.

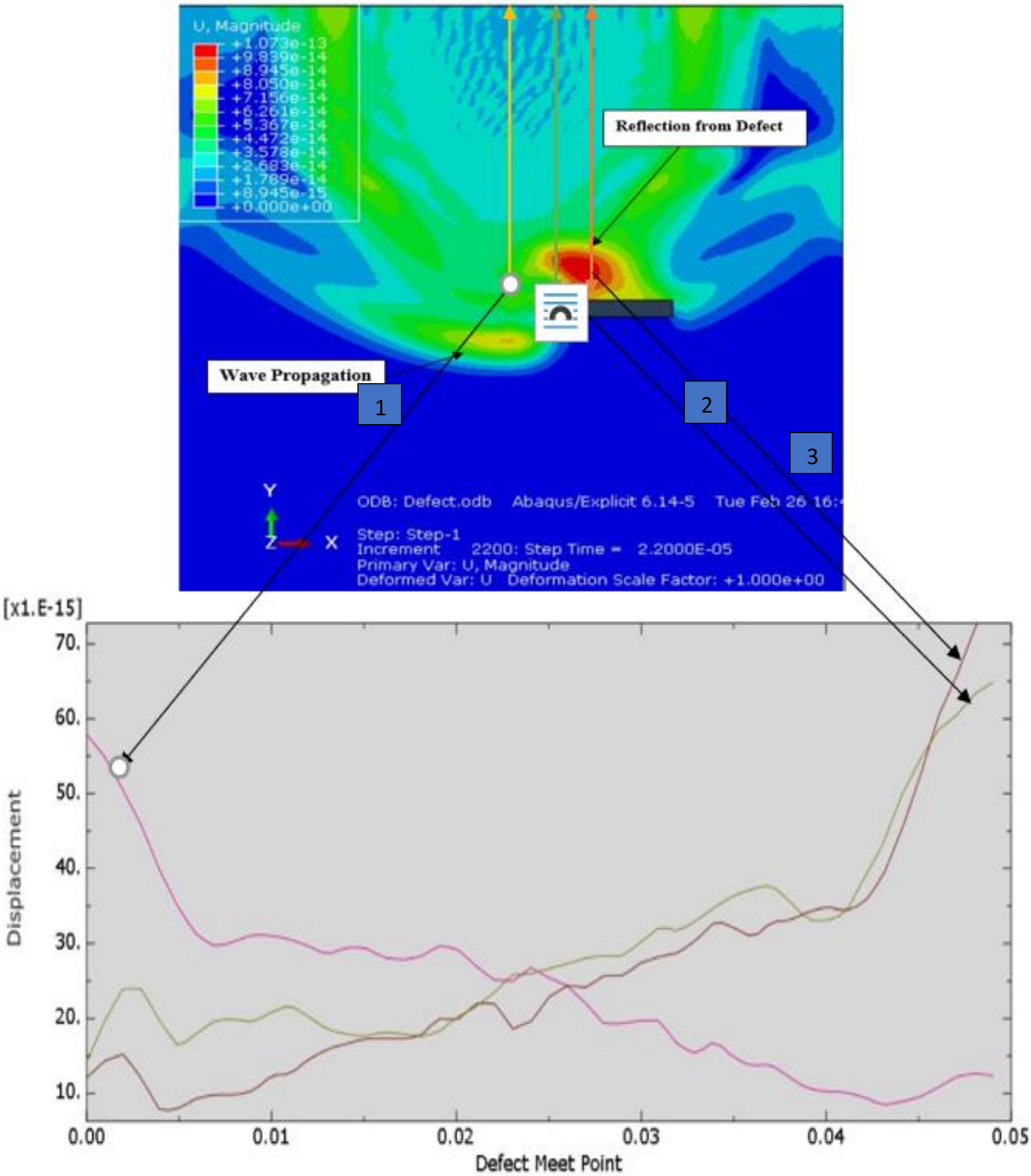


**Fig 38**. Displacement of wave distribution path on defect zone.

### 4.3 Conclusion of analysis using the finite element method

The sample was modelled in computer-aided design for the purpose of analysis. The honeycomb structure was designed as different layers and was assembled in computer-aided design. Using the Finite Element method, the delamination type defect on the composite layer was created artificially and the wave propagation of the composite material without and with defect was observed with respect to time. The 2D finite element model was designed for simple analysis. The wave is excited from excitation zone which contains 13 elements, excitation zone is the transducer.

The excitation sets as seven elements cover the defect region and 6 elements were covers the defect-free zone and the remaining 7 elements were placed in the defect zone. Using the finite element method, the wave interaction with the defect was analysed. The 5Mhz bulk waves propagate through the composite carbon fiber layer.

The part of the wave that meets the defects scatters with respect to the defect and reflects back to the top and the part of the wave that does not meet with the defect propagates along the bottom layer and is reflected back to the origin. The displacement distribution of ultrasonic wave versus defect meets distance. The energy loss of sound energy along the longitudinal direction has been plotted and drawn the graph. The graphs are plotted with defect model and without defect model.

## 5. Experimental analysis of defects on carbon fiber sandwich material

This research focused on the impact damages on honeycomb carbon fiber sandwich material. The impact damages on composite honeycomb structure tend to develop the delamination. Internal deformities can be identified and measured when an appropriate technique is used. **Fig 39** shows the honeycomb carbon fiber sandwich sample and scan system.

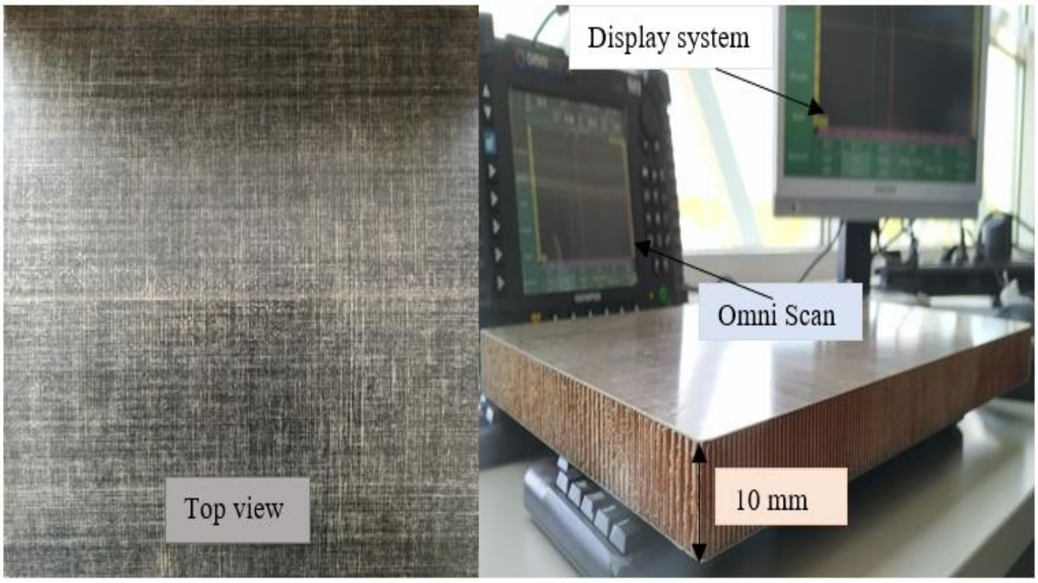


**Fig 39**. Carbon fiber honeycomb sandwich sample.

There are no radiation effects in the ultrasonic examination as in the case of radiography and is less complex. The abnormalities like delamination, impacts damages, cracks, and deformities can be recognized. The investigation was performed using a single transducer and phased array with the frequencies 3.5 MHz and 5MHz. The feasibility of detecting defects on a sample in the results is to be presented.

### 5.1 Transducers

The investigations are carried out using two types of transducers, Single beam transducer, and linear phased array transducer. While each transducer having its own unique nature to identify the flaws in ultrasonic testing. The table 11 shows transducer specifications used for the experimental set-up.

Table 11. single element transducer specifications.

| **S.no** | **Transducer specifications** | |
|---|---|---|
| 1. | Transducer type | Single |
| 2. | Part number | V126 |
| 3. | Serial number | 956892 |
| 4. | Designation | Contact |

| | | |
|---|---|---|
| 5. | Frequency | 5 MHz |
| 6. | Element size | 0.375-inch dia |
| 7. | Energy | 100 volts |
| 8. | Damping | 50 ohms |
| 9. | Shape | Spike |
| 10. | Gain | 21 dB |

In linear array transducer, the array consists of many small piezoelectric elements, each of which can be pulsed independently. By varying the timing, for instance by pulsing the elements one by one in sequence along a row, a pattern of constructive interference is set up that results in a beam at a set angle. In other words, the beam can be focused and steered electronically. The data from multiple beams are put together to make a visual image showing a slice through the object. More piezoelectric elements allow a higher resolution of the transducer array**.** Table 12 shows the linear array transducer properties.

Table 12. Linear transducer array properties

| **S.no** | **Transducer specifications** | |
|---|---|---|
| 1. | Transducer type | Linear array |
| 2. | Frequency | 5 MHz |
| 3. | Wave direction | Longitudinal |
| 4. | No. of elements | 8 |
| 5. | Thickness of the wedge | 3.1 cm |
| 6. | Gain | 20 dB |
| 7. | Focal depth | 35 mm |
| 8. | Type of array | Near field |

### 5.1.1 Single transducer inspection

The experimental setup of the single element transducer has been shown in **Fig 40**. The acquired data from the single element transducer is passed on to the measurement system. In the measurement system, the data is analyzed and processed to identify the defects and measure it. This processed data is then sent to the scan view for review.

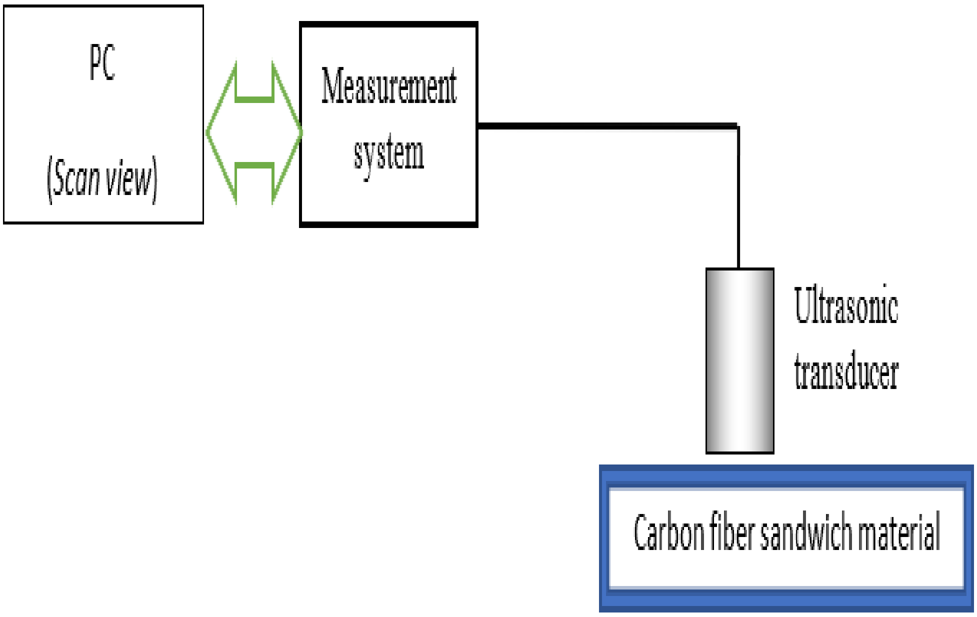


**Fig 40**. Experimental setup of a single element transducer.

**Fig 41** shows the real-time experimental set-up with a single element transducer. The 5MHz transducer placed on the carbon fiber sandwich material and it is connected to the Omni scan measurement system.

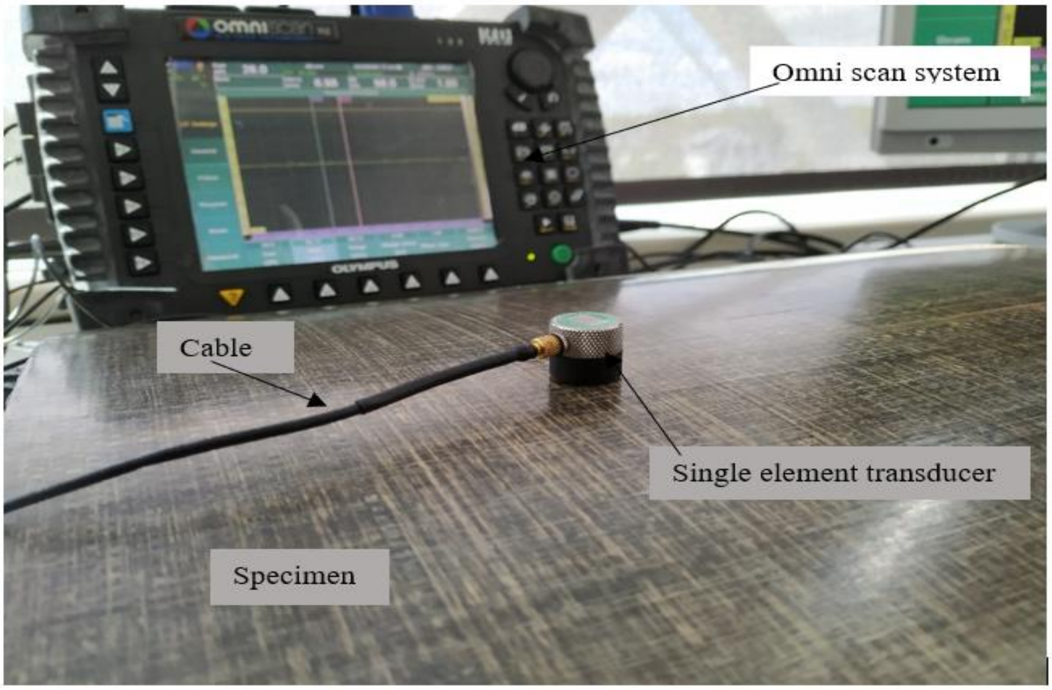


**Fig 41**. Practical experimental set-up using a single element transducer.

**Fig 42** shows the scan view of the single element transducer. The ultrasound wave propagation starts from the single element transducer. The frequency range of the transducer is 5 MHz and its element size is 0.5-inch diameter. The transducer's pulse damping setting is 50 Ohms and receiver attenuation is 54dB and gain is 40dB. The designation of the transducer is in contact mode. The first reflection from the transducer shown in A-scan is said to be a pulse [30].

The reflected wave is shown at the right side. There is no defect detected with single element transducer. If in case there is any defect, the reflection spikes between the pulsar and reflector wave should have been obtained. The amount of sound energy that reflects in between the first wave and third wave give the estimation of defects size and depth.

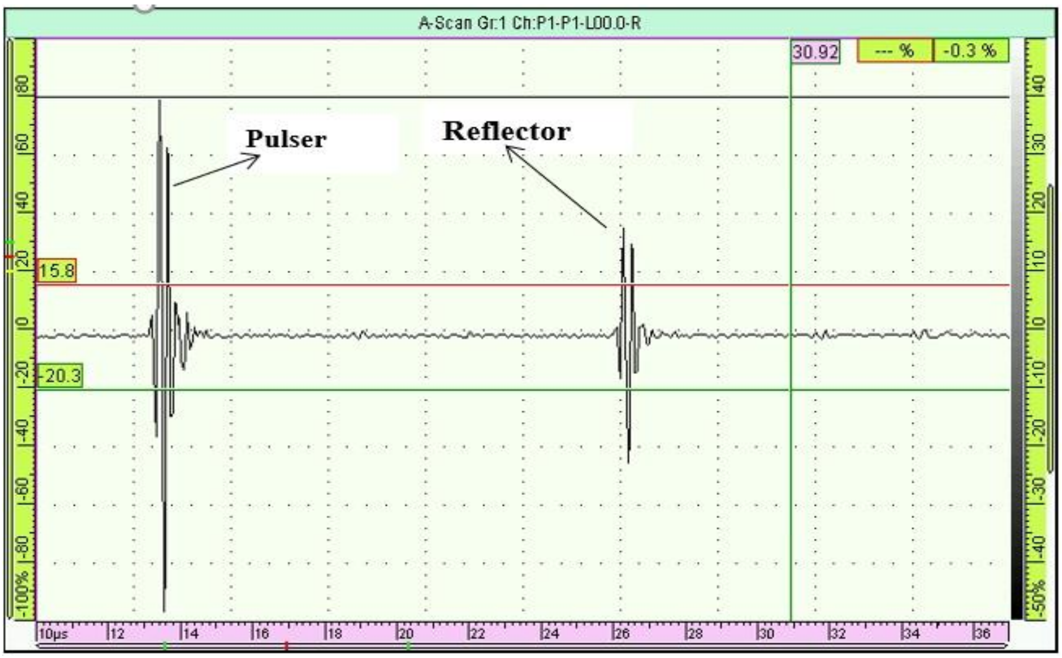


**Fig 42**. Single element transducer wave display on CFSM.

The experimental single element transducer outcome concluded that the impact defects on carbon fiber sandwich were not obtained due to defect placed at a very near surface and the thickness of specimen skin is 1 mm. There are no wedge sets for the single element transducer for wave travel. The spike is not obtained between pulse and reflector. Hence there is no defect shown with a single element transducer.

### 5.1.2 Linear array transducer inspection

The main perspective of the analysis is finding impact damages on carbon fiber sandwich material using a phased array transducer. The specifications of the phased array are the frequency of phased array is 5 MHz, the formation of the wave in the longitudinal direction, the number of elements of the transducer is 128, the type of array is near field and the velocity of the sound for carbon fiber sandwich material is 3200 m/s. The wedge is used to get better contact between the specimen and the transducer. The thickness of the wedge is 3.1 cm.

The individual elements wave fronts that are formed due to time delays in propagation forms steering and is caused by the constructive interference of wave fronts emitted by the transducer array elements at different times. The wave fronts from each element are shown being circular and uniform in amplitude. The energy is concentrated on the axis of each element.

The experimental setup of the linear array transducer is shown in **Fig 43**. The setup from the linear transducer array to the measurement system and it is connected to the computer to display the scan view.

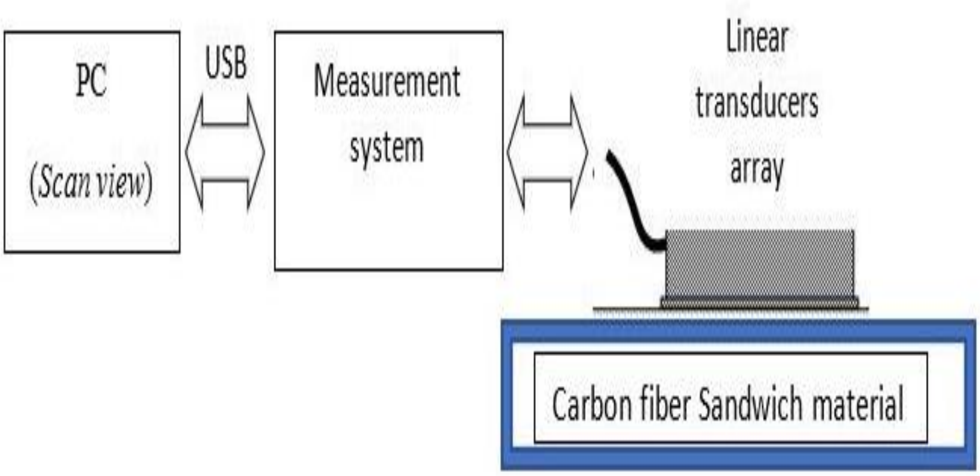


**Fig 43**. The experimental setup of the linear transducer array.

**Fig 44** illustrates that, when the phased array transducer in the place of the normal area of specimen shows no reflection. Because in the absence of damage on the specimen the longitudinal wave travels to the back wall of the specimen and is reflected back to the initial point. The S-scan has been presented without defect presentation.

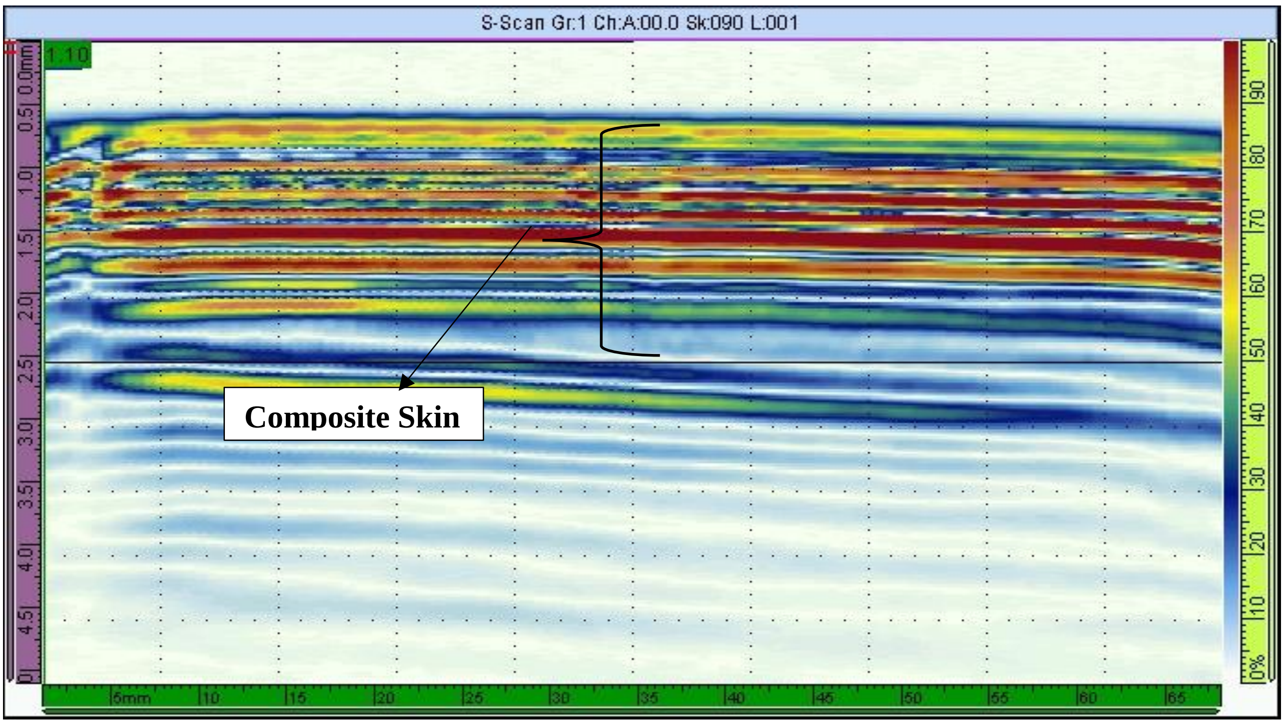


**Fig 44**. The linear transducer array result of carbon fiber sandwich material.

**Fig 45** illustrates that, when the phased array transducer is moved on the impact damage area, the transducer identifies the damage and is shown in the scan view. The variation of both without-damage and with-damage can be seen in **Fig 44** and **Fig 45**. The unique identification of impact damage on carbon fiber sandwich material is obtained in Omni scan measurement system.

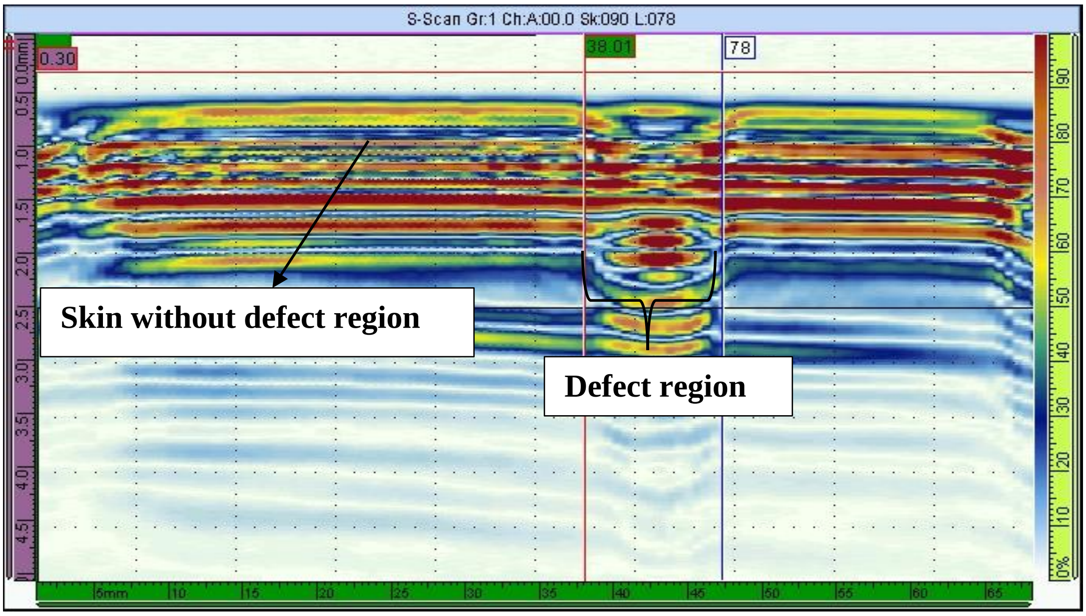


**Fig 45**. Linear transducer array detected damage on scan view.

The practical experiment has been conducted by using the CIVA simulation parameters. The experimental setup is 3.5 and 5 MHz transducer, Omni scan setup and specimen. The transducer is connected to the Omni scan setup and it is placed on the specimen. The contact gel applied to get better wave propagation in order to obtain quality results. The transducer moved gently on the surface of the specimen.

**Fig 46** shows the B-scan view of 3.5 MHz scan results. The abnormalities on the specimen have been shown with different frequency. The difference in defect detecting quality with various frequencies is presented.

The B- scan refers to the image produced when the data collected from an ultrasonic inspection is plotted on a cross-sectional view of the component. It gives scanned Image of the results of an ultrasonic examination showing a cross-section of the test object perpendicular to the scanning surface and parallel to a reference direction. The defect is obtained with 3.5 MHz on carbon fiber sandwich material and the results are presented.

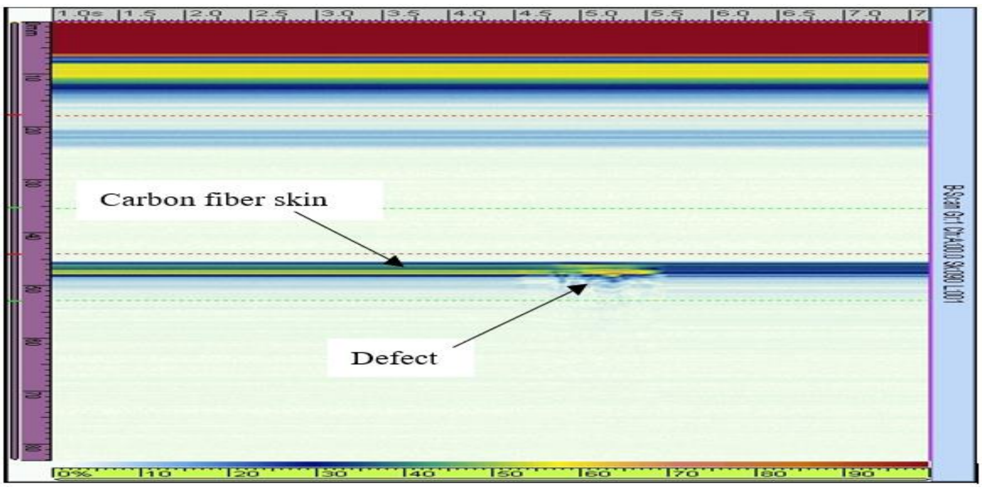


**Fig 46**. Experimental results with 3.5 MHz

**Fig 47** shows the 5MHz Omni scan results with a B-scan view. The 5 MHz frequency shows that the more precise results obtained with 5 MHz frequency. The results are very clear with a linear phased array.

The difference with 3.5 MHz and 5 MHz has been presented and discussed. The wedge is attached to the transducer which helps the transducer to travel some distance, the ultrasound traveling from the transducer to skin is carried to some distance and it gives the better results.

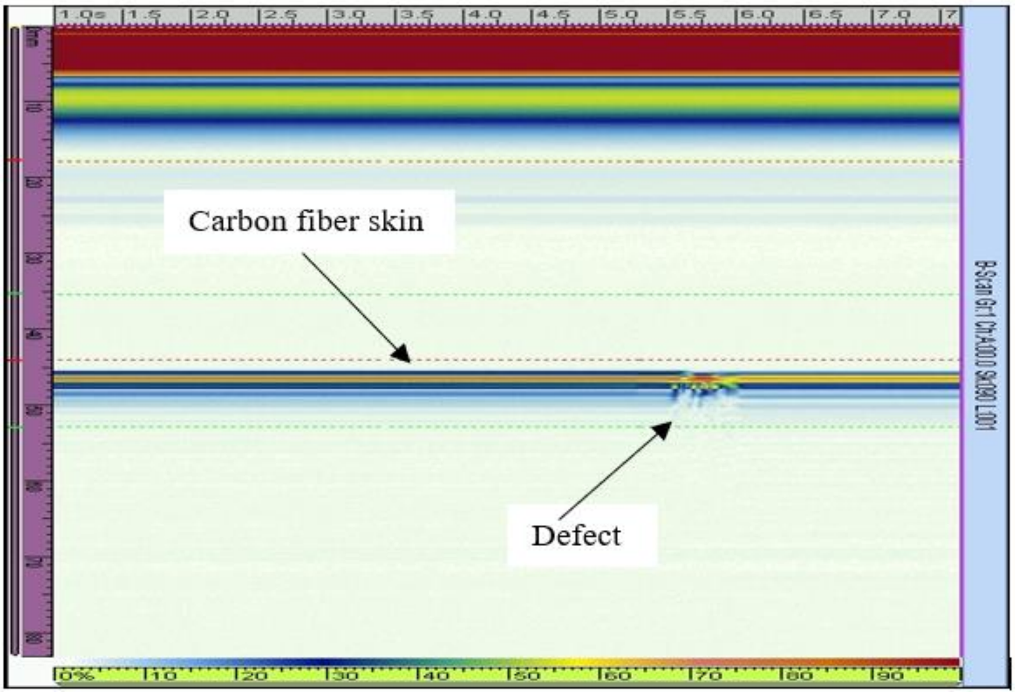


**Fig 47**. Experimental results with 5 MHz

## 5.3 Experimental Conclusions

The practical experiments are conducted with a single element transducer and linear array transducer. The single element transducer was not successful in detecting the defects because of its less coverage area. In linear array transducer, the defects were very well detected as it could overcome the disadvantages of the single element transducer, as it consists of 128 elements which cover a large area of inspection and also the wedge can be attached to it which helps in wave propagation and in easy detection of the defects. The observation concluded that an array transducer is better in detecting impact defects in comparison with a single element transducer. It is the simplest process to detect impact damages with less time.

## 6. Conclusion

In this thesis the non-destructive investigation methods and the analysis of defects in carbon fiber sandwich material were studied. Ultrasonic inspection is the best method to inspect defects on carbon fiber sandwich material by analyzing different NDT methods.

The artificial delamination defects have been created between the skin and honeycomb structure using CIVA software. The 3.5 and 5 MHz phased array transducers selected for the simulation. The 3.5 MHz transducer have 64 elements and it is limited to area coverage and steering capability compare to 5 MHz transducer. The 5 MHz phased array have 128 elements; hence the 5 MHz transducer is the best transducer to inspect the defects on carbon fiber sandwich panel precisely.

The model was designed and analyzed in Abaqus finite element software. The 1 mm thin carbon fiber skin was designed with and without defect. The finite element simulation of the ultrasound wave propagation with and without defect and the wave interactions with defect was achieved.

In this case using the computer-generated parameters the practical experiments have been conducted with single element and linear phased array transducer. The 3.5 and 5 MHz frequencies are used for the inspection. For the inspection of defects on carbon fiber honeycomb sandwich material, the linear phased array transducer is concluded to be the best one compared to the single element transducer. The transducer with 5 MHz gives the precise results compare to 3.5 MHz.

## 7. References


1. **Meltem Altin**, **Karataşa Hasan Gökkayab**.(2018) A review on machinability of carbon fiber reinforced polymer (CFRP) and glass fiber reinforced polymer (GFRP) composite materials- https://doi.org/10.1016/j.dt.2018.02.001
2. **P. Troost. (**2013) Practical application "NDT" techniques on composite materials in aerospace industry- Senior NDT Engineer, TTat Europe bu, 26-11-2013, http://ndt.aero/images/Presentation_26_Nov_2014.
3. **R. Kazˇys** , **A. Demcˇenko**, **E. Zˇ ukauskas**, **L. Mazˇeika**, Air-coupled ultrasonic investigation of multi-layered composite materials - Ultrasound Institute of Kaunas University of Technology, Studentu str. 50, Kaunas LT-51368, Lithuania Available online 6 June 2006.
4. **G**. **Belingardi**, **P**. **Martella**, **L**. **Peron**, Fatigue analysis of honeycomb-composite sandwich beams - Department of Mechanical Engineering, Politecnico di Torino, Corso Duca degli Abruzzi 24, 10129 Torino, Italy Received 1 May 2005; accepted 1 April 2006.
5. **C Nageswaran**, **C R Bird** and **R Takahashi**, Phased array scanning of artificial and impact damage in carbon fibre reinforced plastic (CFRP) - Based on a paper presented at NDT 2005, the 44th Annual British Conference on NDT, Harrogate, UK, September 2005.
6. **K**. **S**. **RAJU**, **B**. **L**. **SMITH**, **J**. **S**. **TOMBLIN**, Impact Damage Resistance and Tolerance of Honeycomb Core Sandwich Panels - Department of Aerospace Engineering, Wichita State University, 1845 Fairmount Wichita KS 67260-0044, USA.
7. **Hesham G**. **Moussa**, **Ana M**. **Martins**, **Ghaleb A**. **Husseini**, Review on Triggered Liposomal Drug Delivery with a Focus on Ultrasound - American University of Sharjah, POBox 26666, Sharjah, United Arab Emirates.
8. **DAVID K. HSU**, Nondestructive Evaluation of Sandwich Structures: A Review of Some Inspection Techniques - Center for Nondestructive Evaluation, Iowa State University Ames, Iowa 50011, USA, journal of sandwich structures and materials, Vol. 11—July 2009.
9. **David K. Hsu**, Nondestructive testing using air-borne ultrasound - Center for NDE, Iowa State University, 1915 Scholl Road, Ames, IA 50014, USA Available online 5 June 2006, doi:10.1016/j.ultras.2006.05.091.
10. **George T, Deshpande VS, Sharp K, Wadley HNG (2014)** Hybrid core carbon fiber composite sandwich panels: Fabrication and mechanical response. Compos Struct 108:696–710. Doi: 10.1016/j.compstruct.2013.10.002
11. **S. Gholizadeh (2016)** A review of non-destructive testing methods of composite materials, PCF 2016, 10-12 February 2016, Paço de Arcos, Portugal www.scribd.com/document/322168075/1-s2-0-S2452321616000093-main.
12. **David K.** NONDESTRUCTIVE INSPECTION OF COMPOSITE STRUCTURES: METHODS AND PRACTICE, HSU Center for Nondestructive Evaluation Iowa State University Ames, Iowa 50011, USA, 17th World Conference on Nondestructive Testing, 25-28 Oct 2008, Shanghai, China
13. **Puw, H Hocheng, H. Y**., Machinability Test of Carbon Fiber-Reinforced Plastics in Milling, Materials and Manufacturing Processes, 1993, 10.1080/10426919308934875, 15322475

14. **GOLDBACH, Rainer FRANKE, IMA Dresden – 2010**, Materials and NDT Applications in Aircraft Component Development Tests Sabine
15. **G. RIEGERT, K. PFLEIDERER, H. GERHARD, I. SOLODOV, G. BUSSE -** 2006, Modern Methods of NDT for Inspection of Aerospace Structures Institute for Polymer Testing and Polymer Science (IKP) –Nondestructive Testing- (ZFP), University of Stuttgart, Stuttgart, Germany.
16. **Wolfgang HILLGER, Detlef ILSE, Lutz BÜHLING Ingenieurbüro Dr. Hillger** – 2012, Practical Applications of Air-Coupled Ultrasonic Technique, Wilhelm-Raabe-Weg 13, 38110 Braunschweig, Germany.
17. **Željko Marušić, Dajana Bartulović, Branko Maković,** Methods to detect and prevent fatigue in ageing aircraft structures - ISSN 1330-3651 (Print), ISSN 1848-6339 (Online) DOI: 10.17559/TV-20140702111704.
18. **Carsten BEINE** – 2010, NDT for CFRP Aeronautical Components A Comparative Study - Fraunhofer Institute for Non-Destructive Testing IZFP, Maria-Reiche-Straße 2, 01109 Dresden, Germany.
19. **Yubei Zhang, Zheng Wang and Guangping**, NDT of aeronautical materials by digital shearography - Guo Beijing Institute of Aeronautical Materials, Beijing 100095, P.R.China.
20. **B. Boro Djordjevic**. 2009, Non-destructive test technology for the composites. The 10th International Conference of the Slovenian Society for Non-Destructive Testing »Application of Contemporary Non-Destructive Testing in Engineering Ljubljana, Slovenia, 259-265.
21. **V. Kappatosa, G. Asfisb, K. Salonitisc, V. Tzitzilonisd, N. P. Avdelidise, E. Cheilakouf, P. Theodorakeasf.** 2016, Theoretical Assessment of Different Ultrasonic Configurations for Delamination Defects Detection in Composite Components. The 5th International Conference on Through-life Engineering Services, Denmark.
22. **C Nageswaran, C R Bird, R Takahashi**. 2005, Phased array scanning of artificial and impact damage in carbon fibre reinforced plastic (CFRP). The 44th Annual British Conference on NDT, Harrogate, UK, September.
23. **Andr´e Cereja, 2015.** Phased Array inspection system applied to complex geometry Carbon Fibre Reinforced Polymer Instituto Superior T´ecnico, Lisboa, Portugal.
24. **FOUCHER, Roman FERNANDEZ, Stéphane LEBERRE, Pierre CALMON.** 2018**.** New tools in CIVA for Model Assisted Probability of Detection (MAPOD) to support NDE reliability studies Fabrice 1 EXTENDE, Massy, France.
25. **V. P. Vavilova,b, Y. Pana , A. I. Moskovchenkoa and A. Čapkac.** 2016**.** Modelling, detecting and evaluating water ingress in aviation honeycomb panels. an Institute of Non-destructive Testing, Tomsk Polytechnic University, Tomsk, Russia.
26. **Ulrich Gabbert, Seyed Mohamad Hosseini, Sascha Duczek**. 2014. Computational and experimental investigation of ultrasonic wave propagation in sandwich panels. Institute of Mechanics, Otto-von-Guericke-University of Magdeburg, Germany.
27. **Ever J. Barbero** – Introduction to composite material design, second edition, CRC Press is an imprint of the Taylor & Francis Group, an informa business, Boca Raton London New York.
28. **Papanaboina**, **M**.**R**.; **Kommanaboina**, **N**.**M**.; **Manimaran**, **H**.**P**.; **Jasiūnienė**, **E**. Inspection of the honeycomb sandwich panel using ultrasonic phased arrays // Transport means 2018: proceedings of the 22nd international scientific conference, October 03-05,

2018, Trakai, Lithuania. Kaunas: Kaunas University of Technology. ISSN 1822-296X. eISSN 2351-7034. 2018, pt. 3, p. 1250-1254. [Scopus]

29. **Papanaboina**, **Mastan Raja**; **Manimaran**, **Hari Prasanna**; **Kommanaboina**, **Naga Manikanta**; **Jasiūnienė**, **Elena**. Analysis of defects in the carbon fiber sandwich material using ultrasonic methods // Pramonės inžinerija - 2018: jaunųjų mokslininkų konferencija, 2018 m. gegužės 10 d.: pranešimų medžiaga / Kauno technologijos universitetas. Mechanikos inžinerijos ir dizaino fakultetas. Kaunas: Kauno technologijos universitetas. eISSN 2538-6727. 2018, p. 132-139. DOI: 10.5755/e01.2538-6727.2018.
30. **Papanaboina**, **Mastan Raja**; **Jasiūnienė**, **Elena**; **Zukauskas**, **Egidijus**. Numerical modelling of ultrasonic wave propagation in carbon fibre material: poster // Open readings 2019: 62nd international conference for students of physics and natural sciences, March 19-22, Vilnius, Lithuania: abstract book. Vilnius: Vilnius University, 2019, P3-33. ISBN 9786090701379. p. 309.

## 8. APPENDIX

Appendix 1. Scientific article of Young scientist conference 2018 on the topic of “Analysis of defects in the carbon fiber sandwich material using ultrasonic methods”

Appendix 2. Scientific article of Transport means 2018: proceedings of the 22nd international scientific conference 2018 on the topic of “Inspection of the honeycomb sandwich panel using ultrasonic phased arrays”

Appendix 3. Poster of Open readings 2019 on the topic of “Numerical modeling of ultrasonic wave propagation in carbon fiber material”

Jaunųjų mokslininkų konferencija

**pažymėjimas**

# PRAMONĖS inžinerija 2018

Nr. V24-11-56

pažymime, kad 2018 m. gegužės 10 d.

**Mastan Raja Papanaboina, Hari Prasanna Manimaran, Naga Manikanta Kommanaboina, Elena Jasiūnienė**

dalyvavo KTU Jaunųjų mokslininkų konferencijoje
„Pramonės inžinerija-2018" ir pristatė pranešimą

**ANALYSIS OF DEFECTS IN THE CARBON FIBER SANDWICH MATERIAL USING ULTRASONIC METHODS**

MIDF Dekanas dr. Andrius Vilkauskas

„Santakos" slėnis, Kaunas

organizatorius

ktu 1922 mechanikos inžinerijos ir dizaino fakultetas

partneris

PTO PAKUOČIŲ TVARKYMO ORGANIZACIJA

# Certificate of Participation

This is to certify that

**Mastan Raja Papanaboina**

has presented a paper titled

**Inspection of the Honeycomb Sandwich Panel Using Ultrasonic Phased Arrays**

at the 22nd International Scientific Conference „**Transport Means 2018**"

held on 3–5 October, 2018 in Trakai (Lithuania)

Chairman of the Conference

Prof. Dr. Zilvinas Bazaras

# OPEN READINGS 2019

## CERTIFICATE OF PARTICIPATION

*This certifies that*

Mastan Raja Papanaboina

*has participated in the 62nd International Conference for Students of Physics and Natural Sciences "Open Readings 2019", which took place on 19-22nd of March in Vilnius, Lithuania.*

Edvinas Skliutas,
Conference Chair

Organising comittee of
Open Readings,
Vilnius University

www.openreadings.eu

Sauletekio Ave. 9-III
LT-10222 Vilnius, Lithuania
info@openreadings.eu